AALTO UNIVERSITY
School of Science and Technology
Faculty of Electronics, Communications and Automation
Department of Communications and Networking

Osman Nuri Can Yilmaz

Self-Optimization of Coverage and Capacity in LTE using Adaptive Antenna Systems

Master's Thesis submitted in partial fulfillment of the degree of Master of Science in Technology

Espoo, 19th February 2010

Supervisor: Prof. Jyri Hämäläinen, Aalto University
Instructor: Dr. Seppo Hämäläinen, Nokia Siemens Networks

AALTO UNIVERSITY **ABSTRACT OF THE MASTER'S THESIS**

Author:	Osman Nuri Can Yilmaz
Name of the Thesis:	Self-Optimization of Coverage and Capacity in LTE using Adaptive Antenna Systems
Date:	19th February 2010 Number of pages: 11 + 60
Department:	Department of Communications and Networking
Professorship:	Radio Communications
Supervisor:	Prof. Jyri Hämäläinen, Aalto University
Instructor:	Dr. Seppo Hämäläinen, Nokia Siemens Networks

In cellular radio networks, the selection of antenna parameters and techniques for antennas plays a key role for capacity and coverage area. Not only network performance is affected by suboptimal network planning but also it is affected by the dynamic radio environment. Therefore, antenna parameters should be adjusted adaptively. Since reacting to the changed situation manually is very expensive and time consuming, The Third Generation Partnership Project (3GPP) introduced the Coverage and Capacity Optimization (CCO) use case for Long Term Evolution (LTE) under the topic of Self-Organizing Network (SON).

This thesis work provides a detailed analysis of the optimization space of antenna parameters and compares different tilt techniques as well as discusses vertical sectorization as a novel capacity optimization approach. The work continues by further focusing on the self-optimization of coverage and capacity using Adaptive Antenna Systems (AAS) on the basis of findings in the previous simulations on antenna parameters.

Evaluations are performed by mapping link-level simulation results into a system level LTE simulator that models antennas in details and propagation in three dimensions.

Keywords: LTE, LTE-Advanced, Remote Electrical Tilt, Mechanical Downtilt, Antenna Modeling, Adaptive Antenna Systems, Self-Organizing Network, Self-Optimization.

Language: English

Acknowledgments

First and foremost I would like to deeply thank my advisors, Prof. Jyri Hämäläinen and Dr. Seppo Hämäläinen for their excellent guidance and valuable comments on simulations and background studies.

I also wish to thank my colleagues from Nokia Siemens Networks (NSN) for their support and encouragement throughout the thesis work.

Furthermore, I would like to thank William Martin, the faculty's language support specialist, for his help while revising the final draft.

Finally, I am immensely indebted to my parents and grandparents for their love and support throughout my everlasting studies, and for the thirst for knowledge they infected me with.

Osman N. C. Yilmaz

19th February, 2010

To my parents and grandparents

Contents

Abbreviations

3D	3 Dimensional
3G	3rd Generation (Cellular Systems)
3GPP	3rd Generation Partnership Project
AAS	Adaptive Antenna System
AC	Admission Control
ACK	Acknowledgement
ADSL	Asymmetric Digital Subscriber Line
ANR	Automatic Neighbor Relation
BLAST	Bell Lucent Layered Space Time Coding
BLER	Block Error Rate
BPSK	Binary Phase Shift Keying
BS	Base Station
CAPEX	Capital Expenditure
CBL	Case Based Learning
CBR	Constant Bit Rate
CDF	Cumulative Distribution Function
CM	Configuration Management
CMC	Connection Mobility Control
CP	Cyclic Prefix
CQI	Channel Quality Indicator
CSI	Channel State Information
DFT	Discrete Fourier Transform
DL	Downlink
DM	Domain Manager
EDT	Electrical Downtilt
EM	Element Manager
EMS	Element Management System
Enb	Evolved Node B
E-UTRA	Evolved Universal Terrestrial Radio Access
E-UTRAN	Evolved Universal Terrestrial Radio Access Network
FFT	Fast Fourier Transform
FM	Fault Management
GBR	Guaranteed Bit Rate
GGSN	Gateway GPRS Support Node
HARQ	Hybrid Automatic Repeat Request
HHO	Hard Handover
HII	High Interference Indicator
HO	Handover
HPBW	Half-Power Beamwidth
ICI	Inter-Cell Interference
ICIC	Inter-Cell Interference Coordination
IDFT	Inverse Discrete Fourier Transform
IFFT	Inverse Fast Fourier Transform
IMT-A	International Mobile Telecommunications-Advanced

IP	Internet Protocol
ISD	Inter-Site Distance
ISI	Inter-Symbol Interference
Itf-N	Northbound Management Interface
Itf-S	Southbound Management Interface
KPI	Key Performance Indicator
LHCP	Left Hand Circular Polarization
LTE	Long Term Evolution
LTE-A	Long Term Evolution-Advanced
MAC	Medium Access Control
MDT	Mechanical Downtilt
MIMO	Multiple Input Multiple Output
MISO	Multiple Input Single Output
MME	Mobility Management Entity
MU-MIMO	Multi User MIMO
NACK	Negative Acknowledgment
NAS	Non Access Stratum
NE	Network Element
NM	Network Manager
NMS	Network Management System
O&M	Operation and Maintenance
OAM	Operations, Administration and Maintenance
OFDM	Orthogonal Frequency Division Multiplexing
OFDMA	Orthogonal Frequency Division Multiple Access
OI	Overload Indicator
OPEX	Operation Expenditure
OS	Operations Systems
PAPR	Peak to Average Power Ratio
PBCH	Physical Broadcast Channel
PCFICH	Physical Control Format Indicator Channel
PCI	Physical Cell Identity
PDCCH	Physical Downlink Control Channel
PDCP	Packet Data Convergence Protocol
PDSCH	Physical Downlink Shared Channel
PHICH	Physical Hybrid Automatic Repeat Request Indicator Channel
PHY	Physical Layer
PM	Performance Management
PMCH	Physical Multicast Channel
PRB	Physical Resource Block
PUCCH	Physical Uplink Control Channel
PUSCH	Physical Uplink Shared Channel
QAM	Quadrature Amplitude Modulation
QoS	Quality of Service
QPSK	Quadrature Phase Shift Keying
RACH	Random Access Channel
RB	Radio Bearer
RET	Remote Electrical Tilt

RHCP	Right Hand Circular Polarization
RLC	Radio Link Control
RLF	Radio Link Failure
RNC	Radio Network Controller
RRC	Radio Resource Control
RRM	Radio Resource Management
RSRP	Reference Symbol Received Power
RX	Receiver
SAE	System Architecture Evolution
SC-FDMA	Single-Carrier Frequency Division Multiply Access
SCH	Synchronization Channel
SFC	Space Frequency Code
SHO	Soft Handover
SIMO	Single Input Multiple Output
SINR	Signal to Interference plus Noise Ratio
SISO	Single Input Single Output
SM	Spatial Multiplexing
SNR	Signal to Noise Ratio
SON	Self-Organizing Network
SRS	Sounding Reference Symbol
SGSN	Serving GPRS Support Node
SU-MIMO	Single User MIMO
TTI	Transmission Time Interval
TU	Typical Urban
TX	Transmitter
UE	User Equipment
UL	Uplink
UMTS	Universal Mobile Terrestrial System
UTRA	Universal Terrestrial Radio Access
UTRAN	Universal Terrestrial Radio Access Network
VET	Variable Electrical Tilt
WiFi	Wireless Fidelity
WiMAX	Worldwide Inter-operability for Microwave Access

List of Figures

List of Tables

1. INTRODUCTION

The third-generation Universal Mobile Terrestrial System (UMTS), based on Wideband Code-Division Multiple Access (WCDMA), has been deployed all over the world. Third Generation Partnership Project (3GPP) launched the Long Term Evolution (LTE) project in November 2004 in order to ensure the continued competitiveness of the UMTS in the future. The specifications of the LTE project are formally known as the Evolved UMTS Terrestrial Radio Access (E-UTRA) and Evolved UMTS Terrestrial Radio Access Network (E-UTRAN).

The radio interface of LTE is based on Orthogonal Frequency Division Multiple Access (OFDMA) [3GPP]. LTE enables admitting higher peak data rates and more users per cell as well as lower control plane latency than previously deployed third generation (3G) technologies. Furthermore, the core network architecture of LTE, referred to as System Architecture Evolution (SAE), is simplified.

Long Term Evolution is further developed to meet the requirements set for International Mobile Telecommunications-Advanced (IMT-A) technologies and is called Long Term Evolution-Advanced (LTE-A). The 3GPP specification in Release 10 is going to be an LTE-A/IMT-A compatible release. LTE-A will have new requirements and new features for the system, for instance, new Self-Organizing Network (SON) use cases to be designed.

Antenna parameter selection and optimization has an important role to achieve maximum capacity and coverage performance in LTE and beyond (LTE-A). For that reason, the LTE framework is adopted for simulations and antenna parameter investigations on the basis of specifications [TR25.814 and TR36.814].

It is noteworthy that previous studies have not comprehensively examined the impact of interactions of antenna parameters such as half-power beamwidth (HPBW), electrical downtilt (EDT), and mechanical downtilt (MDT) with each other in the downlink of LTE. Using the findings in the antenna parameter optimization study as a basis for development, self-optimization algorithms have been developed and tested for the Coverage and Capacity Optimization (CCO) use case and the final results are presented in this thesis.

The results related to the analysis of antenna parameter optimization space, the comparison of electrical and mechanical downtilt optimizations, and the analysis of vertical sectorization have been reported in three conference publications [Yil1], [Yil2], and [Yil3] respectively. It is also planned to submit conference (and journal) papers on the self-optimization of antenna parameters, i.e., Remote Electrical Tilt (RET), antenna azimuth and horizontal HPBW.

1.1. Scope and Goals of the Thesis

This thesis focuses on the downlink performance of LTE networks. Results are analyzed from the system level perspective. The simulation work is divided into five parts as follows:

1. Optimization space of antenna parameters,
2. Comparison of electrical and mechanical downtilt optimizations,
3. Analysis of vertical sectorization,
4. Self-optimization of remote electrical tilt,
5. Self-optimization of the antenna azimuth and horizontal HPBW.

Cell coverage extension, cell capacity enhancement and inter-cell interference (ICI) mitigation provided by optimized antenna parameters are the main objectives in this thesis work.

1.2. Structure of the Thesis

Chapter 2 gives an overview of LTE and LTE-A wireless networks by describing the system architecture and some technical features. Chapter 3 defines SON use cases, discusses the future of SON, and describes the self-optimization algorithms which were developed for the coverage and capacity optimization use case. Chapter 4 defines antenna parameters and describes their modeling details. Chapter 5 presents simulation results and findings. Chapter 6 summarizes the work and draws conclusions. Appendix gives further information on the modeling of system level LTE simulator, the simulation scenarios and the main assumptions.

2. LONG TERM EVOLUTION

2.1. Introduction

Long Term Evolution is a new technology in which radio interface is designed based on OFDMA in the downlink (DL) and Single Carrier – Frequency Division Multiple Access (SC-FDMA) in the uplink (UL) by 3GPP [3GPP]. The work of 3GPP on the evolution of the 3G mobile system is aimed at achieving additional substantial leaps in terms of service provisioning and cost reduction. 3GPP has concluded a set of targets and requirements for Long Term Evolution in Release 8, on the basis of the LTE feasibility study [TR25.9121], and the LTE requirements document [TR25.913], such as:

- LTE will admit higher peak data rates and more users per cell as well as lower control plane latency than currently employed 3G technologies.
- Radio technology is based on OFDMA and it applies sophisticated scheduling and multi-antenna methods.
- Also, LTE network architecture is simplified so that networks can meet requirements set by the anticipated explosion of data traffic volume, the quest for low latency and the hopes of simple, cost effective operation.

By means of simplified network architecture in LTE, the Operation and Maintenance (O&M) subsystem supports the management of centralized remote applications, with planning, measurements, and optimization processes, using computer-aided tools. What is more, the new SON paradigm automates these functions with localized, distributed, centralized and hybrid architectures. These automated functions are designed for a self-organizing behavior, reacting dynamically with the variation of network parameters and performance indicators, optimizing the overall performance and quality.

2.2. System Architecture

System Architecture Evolution, standardized by 3GPP, increases data plane efficiency and minimizes the number of nodes with respect to the second and third generation systems. Intermediate nodes such as the Radio Network Controller (RNC), the Serving GPRS Support

Node (SGSN) and the Gateway GPRS Support Node (GGSN) are removed and replaced by the SAE Gateway (GW), for the reduction of inter-node data traffic delays.

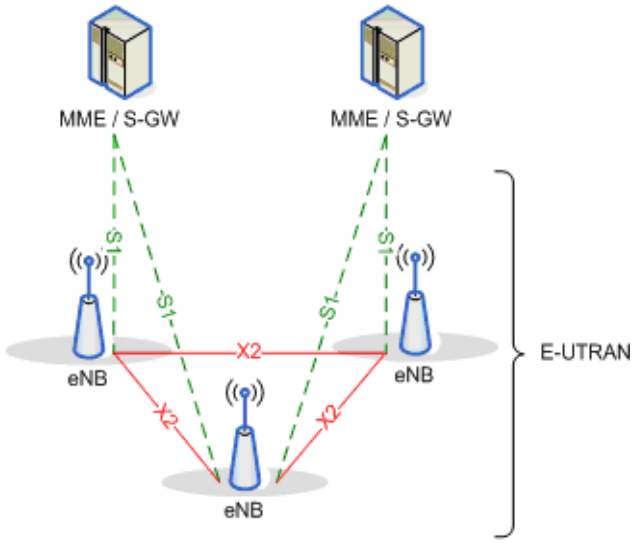

Figure 1. LTE Radio Access Network (RAN) architecture [TS36.300]

In SAE, the central control functions of the RNC are distributed between the evolved Node B (eNB) and the Mobility Management Entity (MME) as eNBs are able to communicate with each other using a new logical inter-eNB interface, called X2 as shown in Figure 1. Thus, the eNB has more control functions than a 3G Node B. The S1 interface is a multiple interface that connects a pool of eNBs to a pool of mobility management entities and gateways.

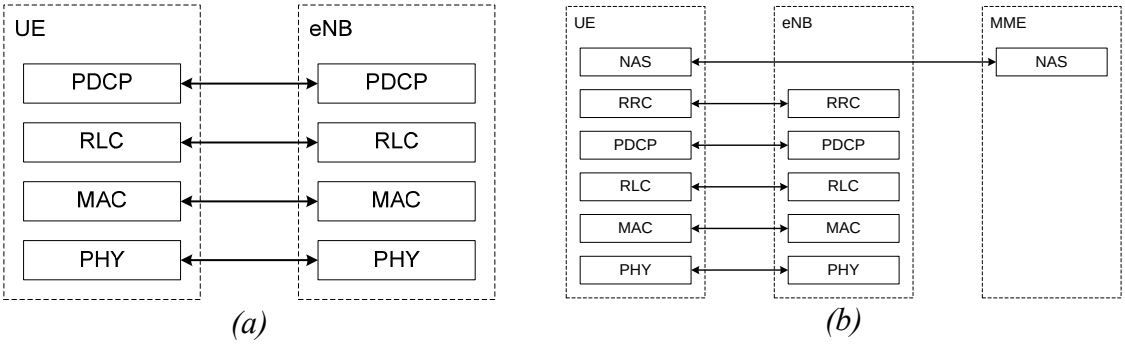

Figure 2. Use- plane (a) and Control-plane (b) protocol stacks [TS36.300]

Since an LTE/SAE network is all-IP, previous transcoding delays are avoided. The eNB incorporates the radio protocol terminations in the user plane shown in Figure 2.a (PDCP / RLC / MAC / PHY) and the control plane shown in Figure 2.b (PDCP / RRC / RLC / MAC /

PHY) towards the User Equipment (UE). The Non Access Stratum (NAS) is the only radio control protocol layer that is terminated in the MME.

3GPP reference model [TS32.101] introduces several interfaces from Operations Systems (OS) to Network Elements (NEs) as follows:

- Itf-S is the vendor specific interface between the Network Elements and the Element Manager (EM), shown as interface 1 in Figure 3.
- Itf-N is the standardized open interface between the Element Manager and the Network Manager (NM), shown as interface 2 in Figure 3. Itf-N facilitates multi-vendor management.
- Itf-P2P is the interface between the Domain Managers (DM), shown as interface 4a in Figure 3.

The functions of SON can reside in NM, EM or NE, depending on use case, through appropriate interfaces which are shown in Figure 3.

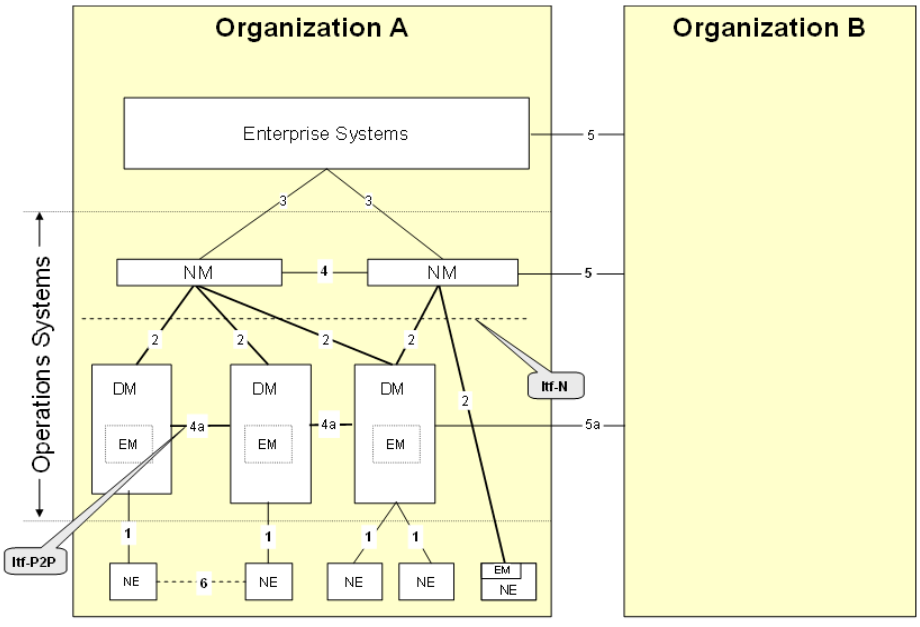

Figure 3. Management reference model [TS32.101]

2.3. Overview of Air Interface in LTE

One of the main changes in LTE compared to 3G is the use of multiple transmission schemes in the air interface. LTE is designed to be based on OFDMA in the downlink, whereas the uplink air interface is based on SC-FDMA. The transmission scheme details are given on the basis of the recently published books about LTE technology [Hol and Les] and 3GPP specifications.

2.3.1. Multiple Access Technology in Downlink: OFDMA

Orthogonal Frequency Division Multiple Access is a variant of Orthogonal Frequency Division Multiplexing (OFDM). It performs well in frequency selective fading channels and provides a feasible and affordable solution with its low-complexity in the implementation as well as allows high spectral efficiency by means of compatibility with advanced receiver and antenna technologies. Hence, it is chosen for the DL of E-UTRAN as selected before in wireless technologies, such as WiFi, WiMAX; and wired technologies, for example, ADSL and ADSL2+.

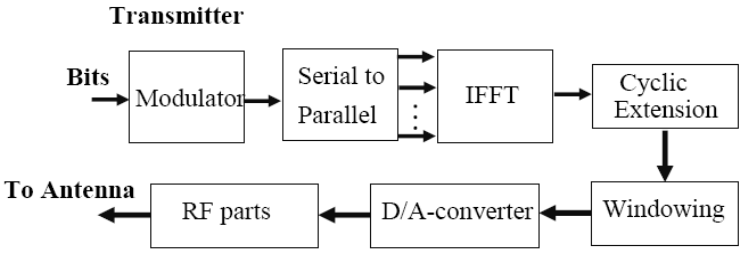

Figure 4. OFDMA transmitter with windowing [Hol]

The main principle of OFDMA is based on the use of narrow, mutually orthogonal subcarriers. At the transmitter side, a group of subcarriers is allocated to each user depending on its data rate. Each Physical Resource Block (PRB), which consists of twelve subcarriers in LTE, is modulated with a conventional modulation scheme (e.g., QPSK, 16QAM, or 64QAM). An Inverse Fast Fourier Transform (IFFT) block is used to move the modulated signal from frequency domain representation to time domain representation after the serial to parallel conversion. To avoid Inter-Symbol Interference (ISI), the transmitter inserts a Cyclic Prefix (CP), which is longer than the channel impulse response, between the symbols. Since the OFDMA transmitter may cause spreading of the spectrum due to imperfections, filtering is carried out for shaping the spectral mask (i.e., windowing).

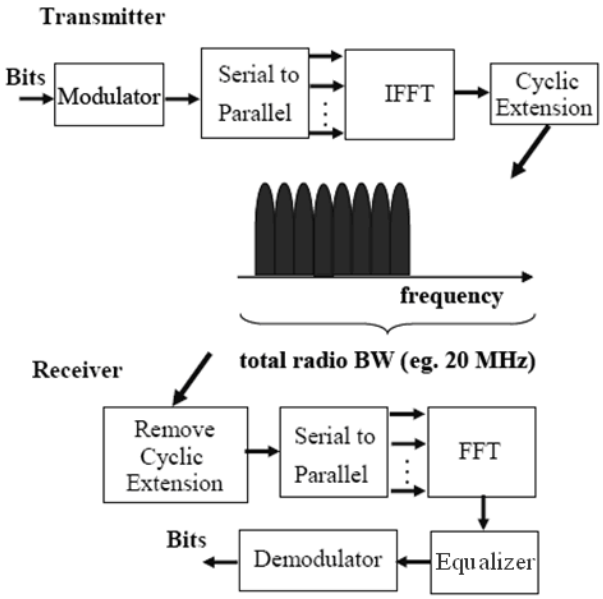

Figure 5. OFDMA transmitter and receiver [Hol]

At the receiver side as shown in Figure 5, the signal is moved from time domain representation to frequency domain representation by a Fast Fourier Transform (FFT) block. Since cyclic insertion and removal is done at the transmitter and the receiver respectively, ISI, caused by the multipath propagation, is no longer a problem unlike WCDMA. On the other hand, the receiver has to deal with the impact of the channel due to the frequency dependent phase and amplitude changes. Thus, the equalization in the frequency domain is performed to remove the channel impact for each subcarrier by multiplying each subcarrier based on the estimated channel response. The downlink reference symbols, which are placed in both time and frequency domains, are used to estimate the channel frequency response interpolating the impact of channel on reference symbols.

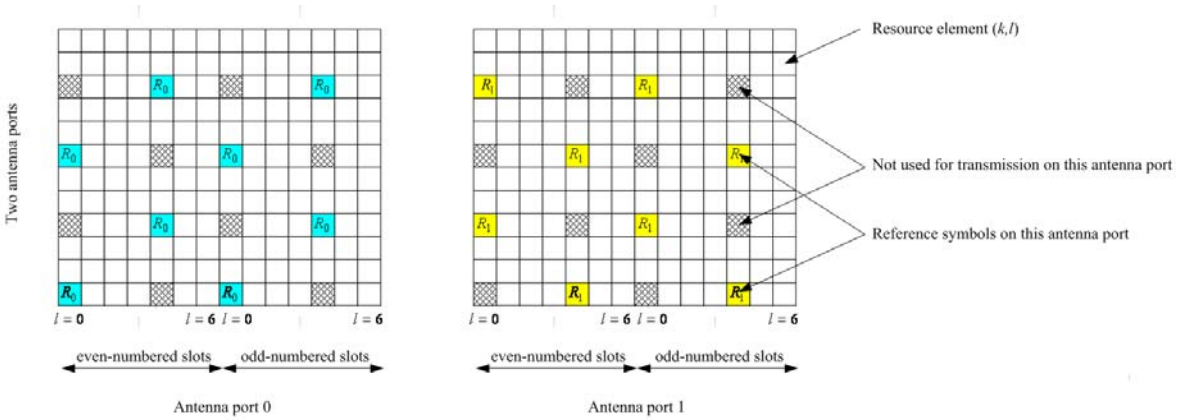

Figure 6. DL reference symbols (extended cyclic prefix, two antenna case) [TS36.211]

2.3.2. Multiple Access Technology in Uplink: SC-FDMA

The Third Generation Partnership Project decided to use SC-FDMA as an uplink transmission scheme due to having a low Peak-to-Average Power Ratio (PAPR), efficient frequency–domain equalization at the receiver side and more flexible frequency allocation with respect to OFDM.

In SC-FDMA, data symbols in the time domain are moved into the frequency domain by using Discrete Fourier Transform (DFT). After the mapping of resources in the frequency domain, the data symbols are converted to time domain symbols by using IFFT. As in an OFDMA system, the CP is inserted periodically but after a block of symbols as the symbol rate is faster in SC-FDMA so that ISI between blocks is avoided and the receiver complexity is reduced.

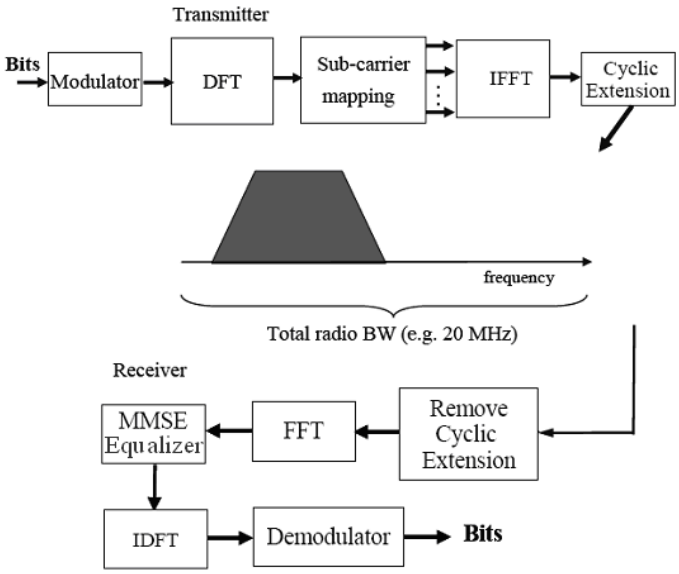

Figure 7. SC-FDMA transmitter and receiver [Hol]

At the receiver side, the cyclic extension is removed and FFT is applied respectively as shown in Figure 7. Since the CP is not added after every symbol, ISI may occur between the symbols of the same block. Therefore, the receiver runs the equalizer for each block of symbols. The reference symbols, which are used for channel estimation, are located in the middle of the slot as shown in Figure 8. After the equalization, the operation of Inverse Discrete Fourier Transform (IDFT) at the receiver removes the DFT precoding and transforms the signal to the time domain.

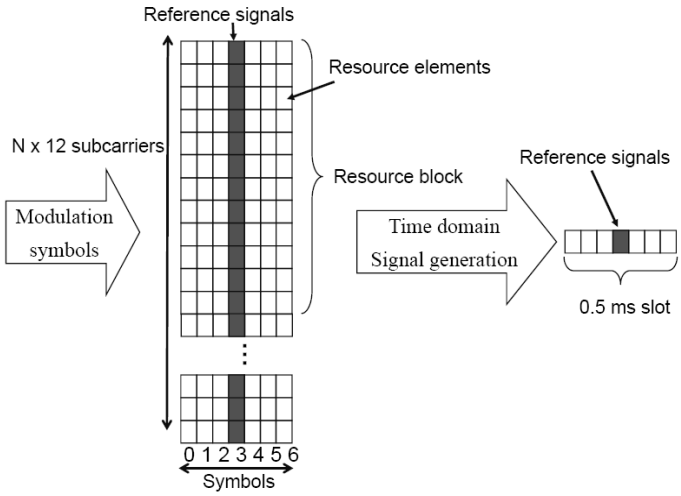

Figure 8. UL reference symbols and resource grid [Hol]

2.3.3. Multiple Antenna Techniques

In modern wireless communication systems, multi-element antenna arrays have been adopted for reliable communications and higher data rates compared to Single Input Single Output (SISO) systems. The major drawback in the deployment of the Multiple Input Multiple Output (MIMO) systems is the increased hardware complexity and the cost due to expensive RF chains (e.g., low noise amplifiers, analog to digital converters). On the other hand, the increasing demand for higher data rates and the reducing capital expenditures (CAPEX) make MIMO technology more favorable from the operator's point of view. Hence, the first release of LTE standards covers up to 4 antennas. Furthermore, LTE-A is going to support up to 8 antennas in order to achieve IMT-A targets.

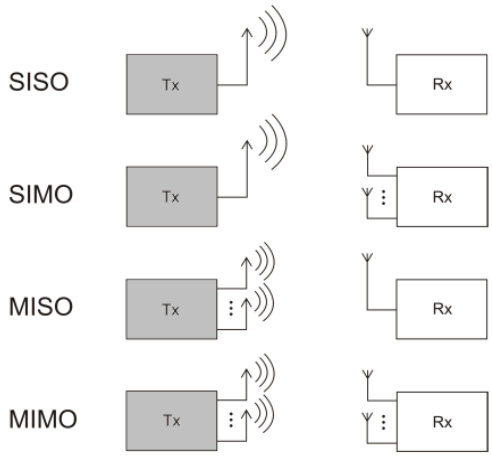

Figure 9. Basic modes in multiple antenna systems

MIMO technology includes different techniques: Spatial Multiplexing (SM) so that multiple data streams are transmitted and received, for instance, Single User (SU) – MIMO and Multi User (MU) – MIMO schemes; and transmit diversity in which a single data stream is multiplexed by space time/frequency codes. MIMO SM is a more effective way to increase the user throughput in higher SNR conditions, whereas MIMO Space Frequency Coding (SFC) performs better in lower SNR conditions [Mog]. Therefore, MIMO mode switching is applied to maximize throughput in LTE DL.

The work of Foschini, Telatar, and others [Fos and Tel] has shown that the capacity of wireless systems can be significantly increased by using MIMO techniques. In [Pol], the capacity gain for HSDPA network by means of 2x2 MIMO spatial multiplexing was shown to be about 42% with respect to a SISO system in a macro cellular network environment with 1.5 km inter-site distance (ISD).

In [Mog], the Shannon formulation is modified to match the link level results of 2x2 MIMO Bell Lucent Layered Space Time Coding (BLAST), 2x2 MIMO SFC, 1x2 Maximal Ratio Combining (MRC) and SISO. The link level performance results of different multiple antenna techniques and SISO, which are approximated by using the modified Shannon formula, are used in system level evaluations by mapping those results shown in Figure 10 to the system level performance measurements.

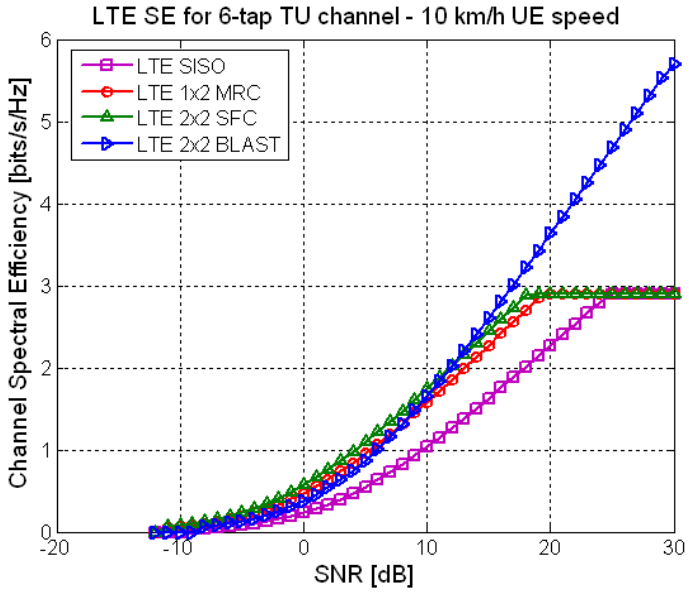

Figure 10. Spectral efficiency vs. SNR for different multiple antenna techniques [Mog]

2.4. Overview of Radio Resource Management in LTE

The Radio Resource Management (RRM) in LTE covers the management and optimization of the radio resource utilization and the network quality. Some of the important features in RRM, for which requirements are given in [TS36.133], are summarized in this section to introduce the basics of LTE RRM.

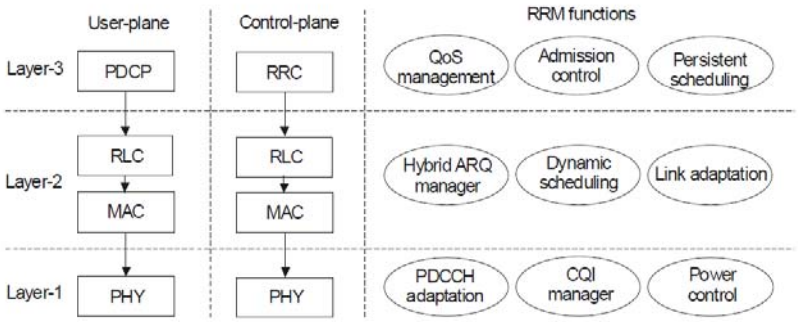

Figure 11. Mapping of the primary RRM functionalities [Hol]

2.4.1. Dynamic Scheduling

Dynamic scheduling is one of the RRM functions of layer 2 as shown in Figure 11 and responsible for the assignment of available uplink and downlink resources in time and frequency domains every Transmission Time Interval (TTI) by allocating PRBs.

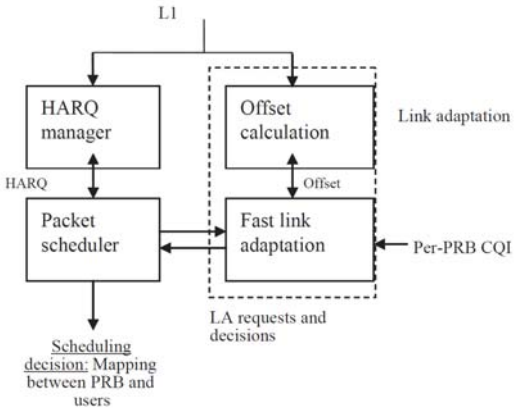

Figure 12. Packet scheduling and link adaptation in the DL [Les]

The dynamic scheduler takes the advantage of the channel variations in time and frequency (i.e., slow and fast fading) so that users under better channel conditions are prioritized in scheduling (i.e., channel aware scheduling). Larger bandwidths provide higher benefits in the frequency domain scheduling because effective coherence bandwidth is less than the system bandwidth [Hol].

In LTE, each cell has its own scheduler and the UE follows the scheduling commands from its serving cell. Scheduling decisions in the uplink and the downlink can be made independently since the downlink scheduling and the uplink scheduling are separated.

2.4.2. Link adaptation

Link adaptation is a fundamental function of the air interface for the efficient data transfer. In the link adaptation of LTE, data rate is dynamically adjusted for each user by changing the type of Modulation and Coding Scheme (MCS) based on channel conditions so that system capacity and coverage performance is improved.

In the downlink, the eNB decides whether a higher or lower level MCS will be used according to the Channel Quality Indicator (CQI). The CQI is an indication of the data rate, which can be supported by the downlink channel, with regard to SINR and the characteristics of receiver.

Outer loop link adaptation is applied to compensate for the CQI measurement errors. It adds a CQI offset to the CQI reports of each UE. Corrected CQI reports are used by the link adaptation for further processing. The CQI offset is controlled by the acknowledgement (ACK) and negative acknowledgement (NACK) responses, provided by the DL Hybrid Automatic Repeat Request (HARQ) mechanism, for the initial transmission of each transport block.

In the uplink, the eNB can directly estimate uplink data rates by channel sounding i.e., using Sounding Reference Signals (SRS) and also controls which modulation and coding schemes can be used in the UL.

The 3GPP specification [TS36.211] defines the following modulation and coding schemes: QPSK, 16QAM and 64QAM in both uplink and downlink directions. On the other hand, 64QAM is not mandatory in the UL except for the UEs with the highest category (Class 5). The number of applicable modulation and coding schemes also depends on the type of channel used as shown in Table 1.

Table 1: Allowed modulation and coding schemes per physical channel

Physical Channel	MCS
PDSCH, PMCH	QPSK, 16QAM, 64QAM
PBCH	QPSK
PDCCH (PCFICH, PHICH)	QPSK
PUSCH	QPSK, 16QAM, 64QAM
PUCCH	BPSK and/or QPSK

Since LTE aims to achieve high peak data rates, it is necessary to use multiple antennas at both terminal and eNB as a basic part of the specifications. However, performances of MIMO modes differ from each other under different SINR conditions, hence MIMO adaptation that can be applied only in the DL switches between transmit diversity and spatial multiplexing modes as well as single TX mode.

2.4.3. Power Control and Inter Cell Interference Coordination

Power control for LTE is standardized within [TS36.213]. In the downlink, the power level can be controlled based on performance indicators, for instance, the indicator of Relative Narrowband Transmit Power (RNTP) per PRB which is signaled to neighboring eNBs through the X2 interface, while in the uplink, terminals use combined open-loop and closed-loop power control. Furthermore, a standardized Inter-Cell Interference Coordination (ICIC) mechanism can mitigate the inter-cell interference in the UL by modifying power settings based on the interference indicators exchanged over the X2, i.e., High Interference Indicator (HII) and Overload Indicator (OI).

2.4.4. Admission Control

Admission control (AC) is one of the RRM functions in layer 3 as shown in Figure 11. AC is in the charge of cell level admission or rejection of the requests for establishment of Radio Bearers (RBs), for example, a paging event, handover (HO) request, or a call establishment request. It evaluates each request with respect to the current cell load and the expected effect of a new bearer on existing connections.

2.4.5. Connection Mobility Control

Connection Mobility Control (CMC) deals with the management of radio resources in relation to idle and connected mode mobility [TS36.300]. In LTE, cell reselection and

handover algorithms are controlled by a setting of parameters (e.g., thresholds and hysteresis values) which determines when the UE should select a new cell or initiate a handover. In active mobility as shown in Figure 13, the handover decision is taken based on the measurements performed by the UE (and eNB). A target cell is selected by the E-UTRAN not by the UE and the core network is only involved when the handover is successful. Packets are forwarded from the source cell to target cell in order to provide lossless handover. What is more, key performance indicators (e.g., neighboring cell load), and policies defined by operator can be taken into account in the eNB for selecting the target cell.

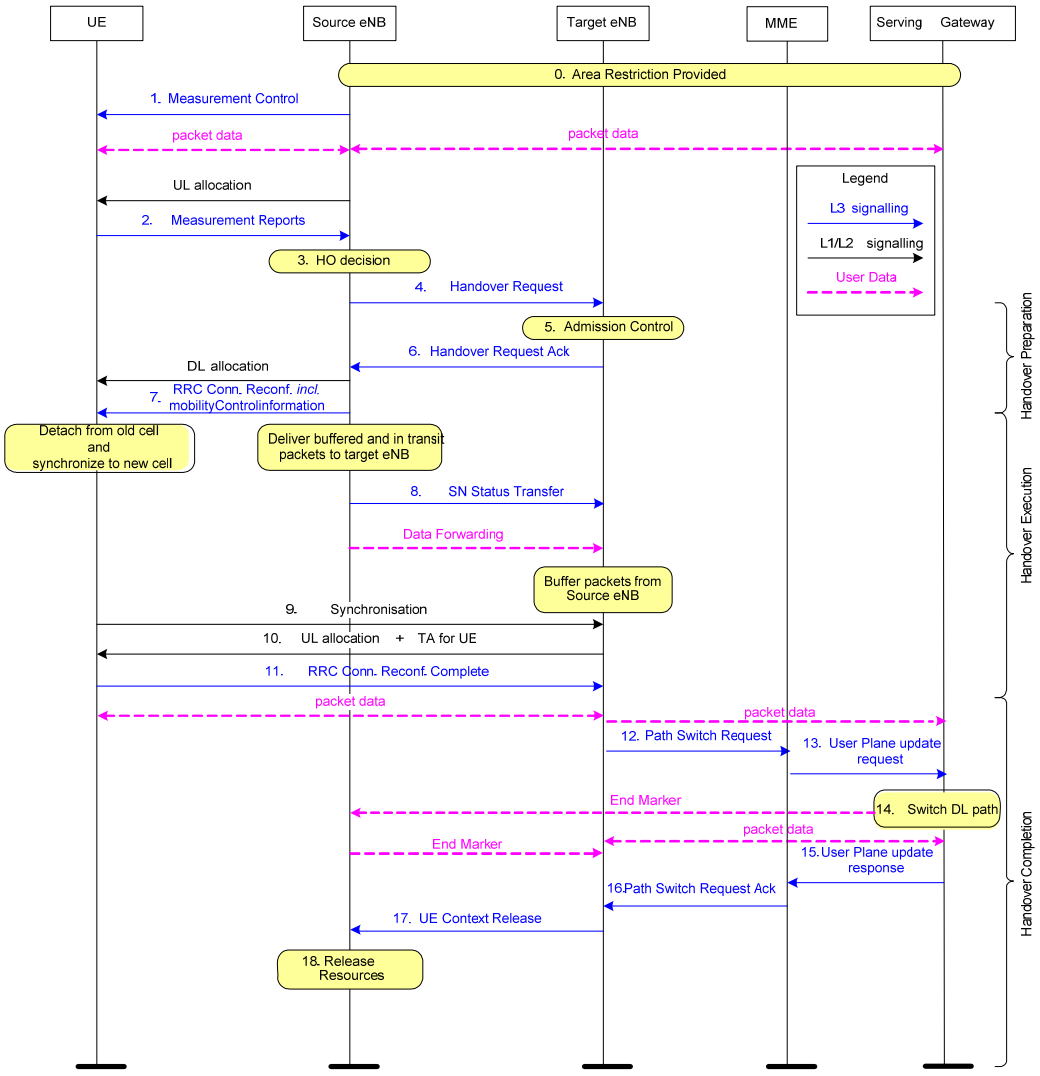

Figure 13. Basic HO process (Intra-MME/Serving Gateway) [TS36300]

3. SELF-ORGANIZING NETWORK

3.1. Introduction

The Self-Organizing Network is of vital interest to operators who strive to minimize capital expenditures and operational expenditures (OPEX) by introducing self-configuring and self-optimizing mechanisms as mentioned in [Soc, NGMN1, and Dot].

The main drivers for automating processes in a mobile network operation are as follows:

- The complexity and the large quantity of parameters in current networks require a lot of effort in the optimization processes, for instance, O&M functionality, drive tests and interface trace analysis, to achieve optimal performance.
- When introducing LTE, it is expected that in many zones, at least three mobile network technologies will be operated in parallel (2G, 3G and LTE/SAE).
- The home eNBs that could be deployed in large quantities should have deployment and O&M processes which are highly automated, nearly plug and play, without the commissioning of installers.

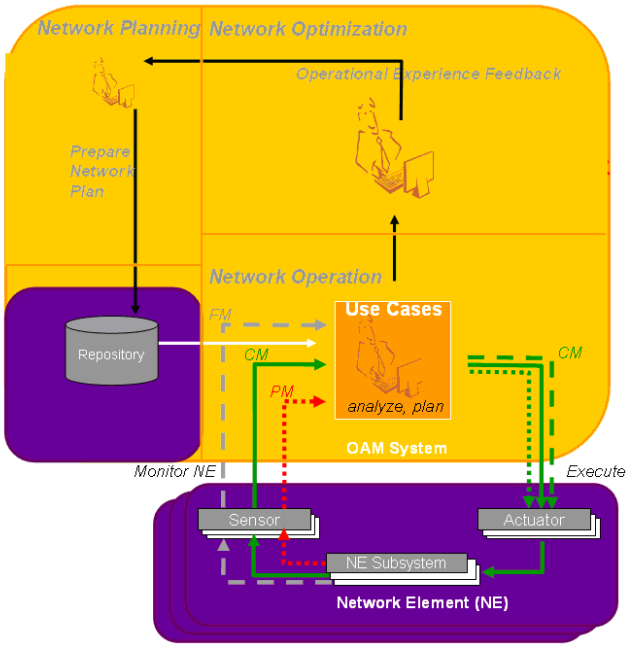

Figure 14. The status of network operation before SON [NGMN2]

In Figures 14 and 15, the status in 3G networks and the status of O&M after including the SON paradigm are presented respectively. In the older status, a network operator continuously monitors the network performance and alarms together with network settings. Network configuration is re-planned by human operator based on analyzed data. Since there are complex operations related to network management in OAM, i.e., Performance Management (PM) that collects performance measurements from the network elements, Fault Management (FM) which is responsible for alarms, and Configuration Management (CM) that is needed for setting parameters in the network elements), errors may be induced by humans, such as a technician.

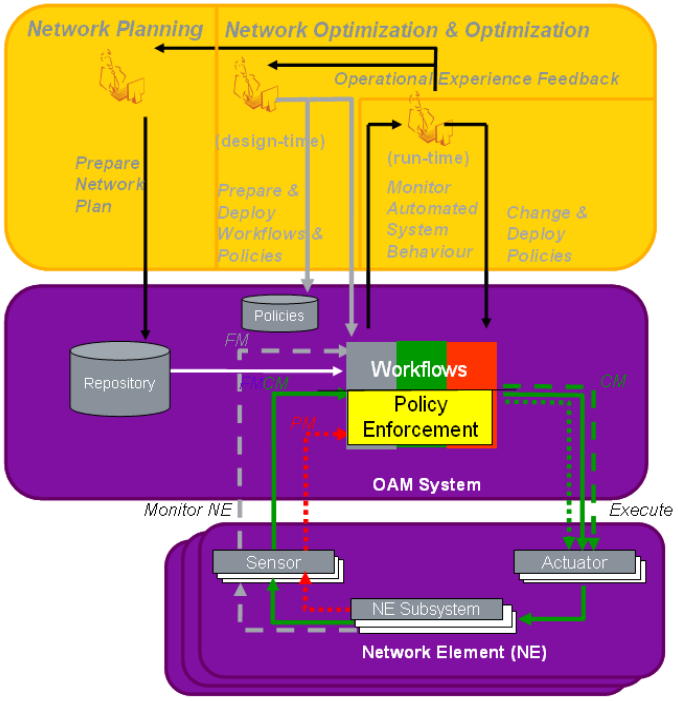

Figure 15. The status of network operation with SON [NGMN2]

SON can be used to reduce OPEX by reducing manual workload. The current vision for SON is to have a stepwise approach by minimizing human interaction in operational procedures and increasing automation in the network elements, domain manager, and/or management system. SON shifts human effort to higher management level, as seen from Figure 15, so that the human operators' role is limited to supervise SON processes and intervene, if needed, as well as to design and decide policies for SON functions. The actual management loop becomes closed and automatic. Therefore, it is expected to provide an OPEX saving. The human operator can always overrule the configurations made by the SON. If any re-

configuration is performed autonomously, THE SON should provide the operator with a full understanding of the new configuration, and allow the operator to revert to the original configuration.

3.2. Optimization Architectures in SON

SON architectures can be divided into four classes according to the location of optimization algorithms: centralized SON, distributed SON, localized SON and hybrid SON. Figure 16 depicts the applicability of localized, distributed and centralized SON, depending on the number of involved cells and the network reaction times. In practice a hybrid SON is required, in which all three kinds of approaches are in use simultaneously coping with different needs for different use cases in a self-coordinated manner.

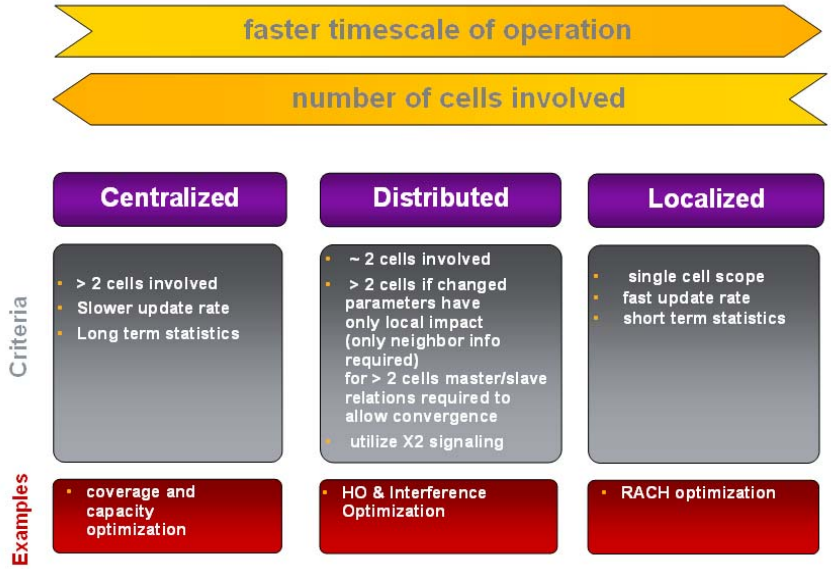

Figure 16. Applicability of centralized, distributed and localized SON

3.2.1. Centralized SON Architecture

Centralized SON is a mechanism, where a large number of cells can be involved in the optimization, having slower update rates based on long-term statistics. In centralized solutions, SON functionality resides in a small number of locations, at a high level in the architecture, for instance, the network management or Element Management System (EMS), depending on the requirements (e.g., multi-vendor capabilities). The use cases in centralized SON such that it requires many cells to be treated simultaneously, e.g., if the transmission

power/antenna tilt of a base station is altered, it has to be taken into account in the neighboring cells due to the changed interference situation. In the case of centralized SON, optimization algorithms are executed in the OAM system. Since all SON functions are located in OAM systems, it is easy to deploy them. On the other hand, there is low support for optimization among different vendors as each vendor has its own OAM system.

3.2.2. Distributed SON Architecture

Distributed SON is applied in the processes that a few cells (e.g., 2 cells) are involved in the optimization, for instance, altered parameters have only a local impact (i.e., only information exchange between neighbors is required). Information between the cells involved is exchanged over X2 interfaces. As X2 is the interface between neighboring eNBs, it is not feasible to relay data from eNBs to other eNBs far apart from each other. Distributed solutions involve some load on the interfaces, e.g., X2, and need to be checked for stability and convergence. Hence, particular use cases where typically around two cells are involved in the optimization process, are predestined for a distributed approach (e.g., two cells optimizing their HO offset values). In the case of distributed SON, optimization algorithms are executed in eNB. In distributed architecture, SON functionality resides in many locations at a low level in the architecture. Since all SON functions are relocated in the eNB, a lot of deployment work is required. It is also difficult to support complex optimization schemes, which require the coordination between many eNBs. However, it is easy to support those cases that only concern one or two eNBs and require quick optimization responses.

3.2.3. Localized SON Architecture

Localized SON is applicable to the processes where only a single cell is involved. Use cases for localized SON require a fast response time and have single cell scope as they do not have significant impact on their neighbors, e.g., Random Access Channel (RACH) optimization.

3.2.4. Hybrid SON Architecture

A hybrid SON architecture is needed as all different kinds of use cases exists in practice at the same time with different scopes. In Hybrid SON, part of the optimization algorithms are executed in the OAM system, whereas others are executed in eNBs. Simple and quick optimization schemes are implemented in eNBs and complex optimization schemes in the

OAM system. Thus, hybrid SON architecture is flexible to support various optimization use cases that have different requirements. It also enables the optimization between different vendors through X2 and Itf-N interfaces.

3.3. SON Use Cases in 3GPP

3.3.1. Self-configuration

Self-configuration covers pre-operational phases of network elements such as network planning and deployment in order to reduce capital expenditures. [TR36.902] defines self-configuration use cases as follows:

- Automatic Neighbor Relation (ANR) function,
- Automated configuration of Physical Cell ID (PCI).

Moreover, [TS32.500] describes the following use cases:

- Self establishment of a new eNB in the network,
- Self-configuration and self-healing of eNBs.

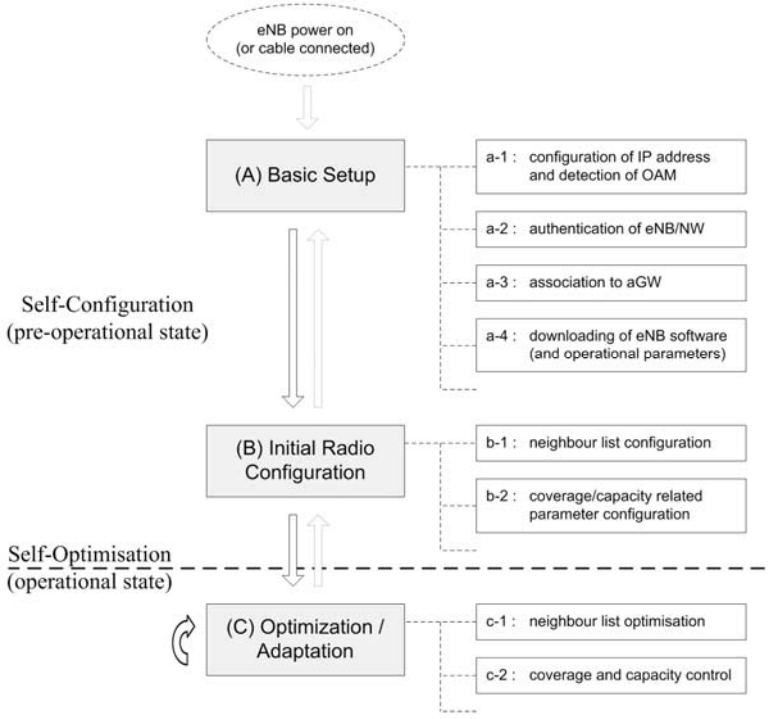

Figure 17. Self-configuration and self-optimization of eNBs [TS36.300]

3.3.2. Self-optimization

Self-optimization takes place in operational state so that network operators get benefits of the dynamic optimization, e.g., mobility load balancing to make network more robust against environmental changes [Vie] as well as the minimization of manual optimization steps to reduce operational costs. The main use cases in self-optimization are [TR36.902]:

- Coverage and capacity optimization,
- Energy savings,
- Interference reduction,
- Mobility robustness optimization,
- Mobility load balancing optimization,
- RACH optimization,
- Inter-cell interference coordination.

In addition, the following self-optimization use cases are described in [TS32.500]:

- Self establishment of a new eNB in the network,
- Self-configuration and self-healing of eNBs,
- Optimization of parameters due to troubleshooting,
- Continuous optimization due to dynamic changes in the network,
- Optimization of Quality of Service (QoS) related radio parameters.

3.4. Considerations on Release 10 Use Cases

Long Term Evolution is further developed to meet the requirements set for IMT-Advanced technologies and is called LTE-Advanced. The 3GPP specification in Release 10 is going to be an LTE-Advanced/IMT-Advanced compatible release. LTE-A will have new requirements and new features for the system that will require new SON use cases needs to be designed.

The requirements for the further advancements for E-UTRA (LTE-Advanced) are described in [TR36.913]. In LTE-A, power efficiency in the infrastructure and terminal is an essential element. LTE-A is going to cover further enhancements in SON as well, for instance,

- Special care with respect to SON is going to be taken for special deployment scenarios like network sharing,
- Special care with respect to SON is going to be taken for mass deployment scenarios like in the case of home eNBs, i.e., inbound and outbound mobility for home eNode B and problems caused by incorrect behavior of home eNBs,
- Avoiding the need for drive tests,
- Impact on UE complexity and power consumption needs to be taken into account.

Operation and maintenance tasks are going to be minimized to the maximum possible extent. What is more, all the interfaces specified are going to be open for multi-vendor equipment interoperability.

From these requirements initial use cases can be derived, such as:

- Optimization of energy consumption,
- SON in heterogeneous deployments,
- Plug and play self-configuration,
- Mobility related use cases,
- Avoiding drive test / cell outage / coverage hole management,
- In conjunction of LTE-A new features such as local area access (Home eNB), relay stations, enhanced MIMO processing and flexible spectrum use is discussed. These new features imply potential new SON use cases, such as:
    - Self-configuration and optimization of many small nodes,

- Handling of more dynamic network topologies,
- Handling of new ICI and mobility scenarios,
- MIMO mode control and coordination,
- Optimization of spectrum use.

3.5. SON Algorithms

3.5.1. Challenges in Algorithm Development

Algorithm development and implementation is the most vital part in self-optimization due to the challenges in optimization and risks in a live network. Some of the main challenges mentioned in [Dot] are the following:

- There is no clear mapping from a large vector of input data to the root cause of a problem, or a promising strategy to improve the situation.
- Incomplete and partly erroneous information may not be sufficient for the decision.
- Full search approaches are not possible due to the large parameter space.
- Trial-and-error in a live network is prohibitive due to the risk of negative performance impact.

3.5.2. Algorithm for the Use Case of Coverage and Capacity Optimization

In our research, various types of algorithms and methods have been adopted and tested in order to minimize the risks and errors. One of those methods is on the basis of Case Based Learning (CBL) which stores cases or instances in memory and applies these cases directly new situations [Aha, Iba, and Ueh]. CBL1 is an appropriate case based learning technique because of its low complexity in implementation and high accuracy in case of small number of training examples and irrelevant features [Ueh]. In CBL1, all numeric feature values are linearly normalized and *k*-Nearest neighbor algorithm is used as a prediction function [Aha].

Until the minimum number of samples is collected for CBL1, the self-optimization algorithm clusters each cell using predefined criteria to optimize its current antenna parameter θ_{curap} as

defined in (1). Each cluster is assigned to a normalized feature value $KPI_{i,j}$. Key Performance Indicators (KPIs) can be divided into M groups (e.g., coverage and capacity) and each group includes N elements. Weightings of groups and elements, which are denoted by k_i and k_j respectively, have an impact on the change in antenna parameter $\tilde{\theta}_{stepap}$.

$$\tilde{\theta}_{stepap} = \sum_{i=1}^{M}\sum_{j=1}^{N} k_i \cdot k_j \cdot KPI_{i,j}(\theta_{curap}) \tag{1}$$

After initial statistics are evaluated (e.g., 4 steps), a set of *k* cases that are most similar to the given query are retrieved from the memory. The following equation (2) is used to compute the similarity to the input query Q for each case C.

$$Similarity(C,Q) = \frac{1}{\sqrt{\sum_{k=1}^{M}\sum_{j=1}^{N} W_{i,j} \cdot \left(KPI_{i,j}^{C} - KPI_{i,j}^{Q}\right)^2}} \tag{2}$$

where $W_{i,j}$ is the weight assigned for KPI class (feature) $KPI_{i,j}$.

After the computation of similarity, the change in antenna parameter $\tilde{\theta}_{stepap}$ is determined based on the previous decisions in similar cases.

γ_{geo} is the factor that reflects the impact of the antenna directions and geo-locations of neighboring base stations as well as other inputs related to the radio network environment on the antenna parameter step. The step size of antenna parameter θ_{stepap} is limited in order to avoid too aggressive and too slight changes as defined in (3).

$$\theta_{stepap} = \begin{cases} \theta_{\min stepap}, & \left(\gamma_{geo} \cdot \theta_{stepap}\right) \le \theta_{\min stepap} \\ \theta_{\max stepap}, & \left(\gamma_{geo} \cdot \theta_{stepap}\right) \ge \theta_{\max stepap} \\ \tilde{\theta}_{stepap}, & otherwise \end{cases} \tag{3}$$

If the decided value of the antenna parameter θ_{newap} in (4) provides the maximized performance in the cost-function (5) as defined in (6) on the next page, it becomes θ_{optap}.

Local optimization is finalized when a cell fulfills the requirements or achieves its optimal performance. In the case of wrong decision, previous adjustment is retrieved as explained in Figure 18. The weighting parameter $w_{i,j}$ in the cost function (5) can be modified by changing policies of an operator.

$$\theta_{newap} = \theta_{ap} + \theta_{stepap} \tag{4}$$

$$f_{\text{cost}}(\theta_{\text{newap}}) = \sum_{i=1}^{M}\sum_{j=1}^{N} w_{i,j} \cdot KPI_{i,j}(\theta_{\text{newap}}) \tag{5}$$

$$\theta_{\text{optap}} = \underset{\theta_{\text{newap}} \in \theta_{\text{rangeap}}}{\arg\max}\ f_{\text{cost}}(\theta_{\text{newap}}) \tag{6}$$

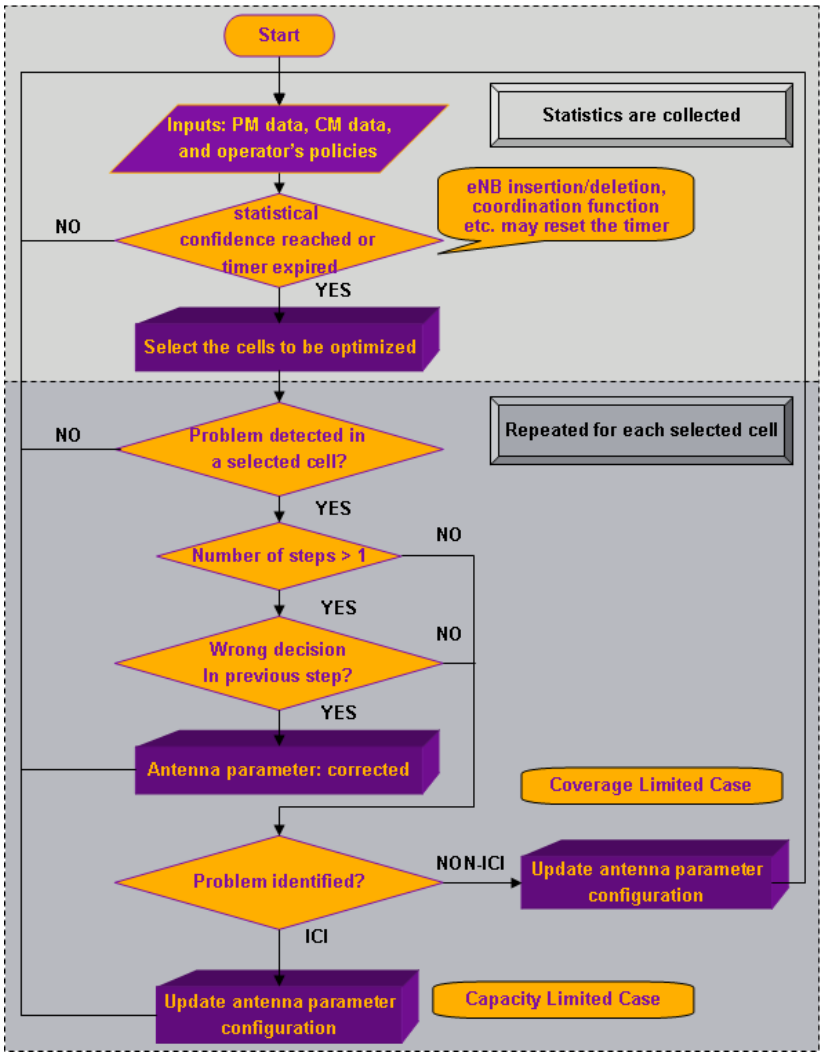

Figure 18. Flow-chart of the algorithm

The algorithm uses global knowledge of the network in terms of KPIs, hence it is called the centralized optimization algorithm. The reason why a centralized approach has been chosen is to strengthen the analysis of the root cause of the problem (e.g., capacity vs. coverage, too much uptilting vs. too much downtilting) and select the cells to be optimized by using (5) with dedicated weighting parameters for prioritization as well as avoiding the changes in the parameters of the cells which may have an impact on each other.

KPIs are a set of selected indicators used for measuring the current network performance and trends. They can be used for prioritizing the corrective actions. On the other hand, action for optimization is taken only if there is a significant problem detected, based on statistically reliable KPI data, with respect to the coverage and capacity performance targets. In busy hours, shorter decision periods (e.g., the period of self-optimization: 1 hour) may be sufficient for making a decision. However, if the number of measurements is not enough during the KPI reporting time interval, the decision period will take longer.

4. MODELING OF BASE STATION ANTENNA PARAMETERS

4.1. Introduction

Dipole and monopole antennas are the most widely used ones for wireless mobile communication systems [Fuji, Jen1, Jen2, Kat1, and Kat2]. At the base station of a cellular radio network, an array of dipole elements is extensively used because of its broadband characteristics and simple construction.

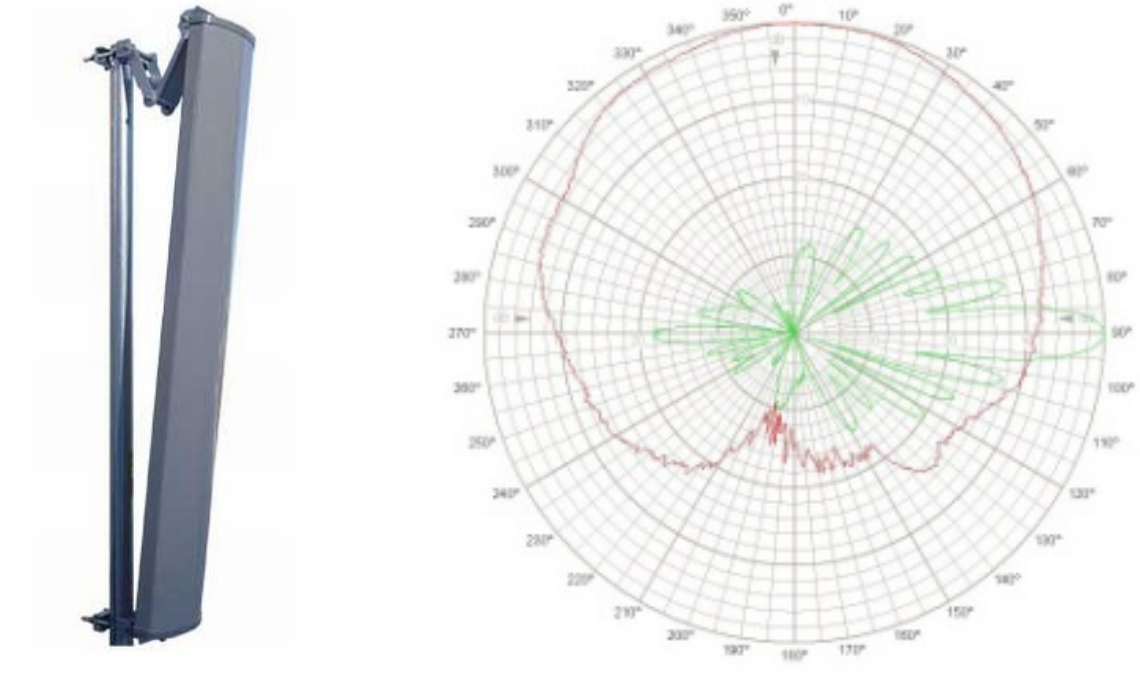

(a) *(b)*

Figure 19. Base station antenna (a) and radiation patterns (b) [Wir]

Base station antennas which have adaptable parameters (e.g., remote electrical tilt and MIMO mode), called Adaptive Antenna System (AAS), will become an integral part of LTE base station platforms for providing better system performance and radio network capacity.

4.2. Antenna Parameters

Even though there is a wide variety of antenna types and geometries, all antennas can be described by a small set of main parameters. In this section, those fundamental parameters based on [Bal, Ell, and Poz], antenna azimuth and tilt for base station antennas are defined.

• **Far-field:** It is the region away from an antenna where the radiated wave takes the form of a plane wave. The criterion, which is commonly used, is $2D^2/\lambda$ where D is the maximum linear transmission of the antenna, and λ is the operating wavelength.

• **Directivity:** The ratio of the radiation intensity U in a given direction from the antenna to the radiation intensity averaged over all directions. The directivity depends on the shape of the radiation pattern. The average radiation intensity is equal to the total power radiated P_{rad} by the antenna divided by 4π .

$$D = \frac{4\pi U}{P_{rad}} \tag{7}$$

• **Efficiency:** Power in the antenna may be dissipated due to conductor loss or dielectric loss. Hence, antenna efficiency η can be defined as the ratio of total power radiated P_{rad} by the antenna to the input power P_{in} of the antenna.

$$\eta = \frac{P_{rad}}{P_{in}} \tag{8}$$

• **Gain:** Antenna gain is the product of efficiency and directivity, but the loss due to conductor loss or dielectric loss reduces the power density radiated in a given direction.

$$D = \frac{4\pi U}{P_{in}} \tag{9}$$

The efficiency and gain characteristics of the antenna are strongly influenced by the frequency of operation [Bal].

• **Half-Power (3dB) Beamwidth:** This term defines the aperture of the antenna. The HPBW is defined by the points in the horizontal and vertical diagram, which show where the radiated power has reached a -3 dB level with respect to the main radiation direction. These points are also called 3 dB points.

• **Input Impedance:** It is defined as the impedance presented by an antenna at its terminals or the ratio of the voltage to the current at a pair of terminals or the ratio of the appropriate components of the electric to magnetic field at a point.

• **Bandwidth:** Bandwidth is defined as the range of frequencies within which the performance of the antenna conforms to a specified standard.

• **Polarization:** Polarization of an antenna refers to the polarization of the electric field vector of the radiated wave. Linear (vertical or horizontal), and circular, i.e., Right Hand Circular Polarization (RHCP) and Left Hand Circular Polarization (LHCP), are the most typical antenna polarizations. Antennas can also be designed to operate with two polarizations, e.g., X polarization widely used in base station antennas.

• **Antenna azimuth:** It is defined as the direction, in degrees referenced to true north, that an antenna must be pointed. The angular distance is measured in a clockwise direction.

• **Antenna tilt:** It is defined as the angle of the main beam of the antenna below the horizontal plane. Positive and negative angles are also referred to as downtilt and uptilt respectively [Sio]. Antenna downtilt can be adjusted mechanically and/or electrically as shown in Figures 20 and 21 respectively.

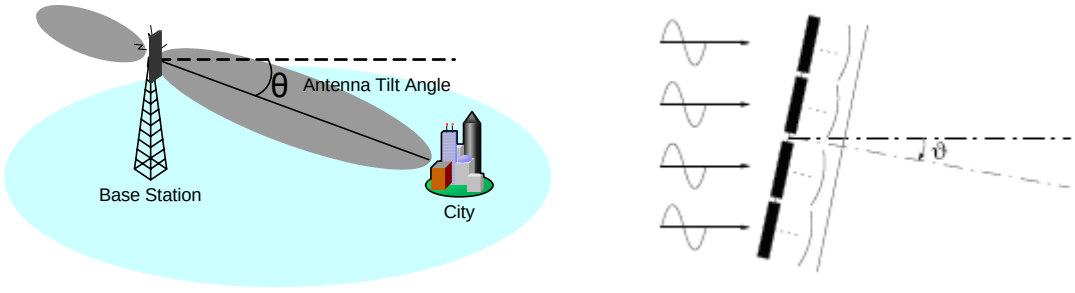

(a) *(b)*

Figure 20. Mechanical tilt [Sio]

There are different existing techniques for electrical tilt such as RET, variable electrical-tilt (VET) and fixed electrical tilt. Usage of RET antennas removes the need for tower climb and base station site visits by controlling electrical tilt angle by NMS so that operational cost is saved. On the other hand, mechanical downtilt is also needed because the electrical tilt range is narrower than the mechanical tilt range.

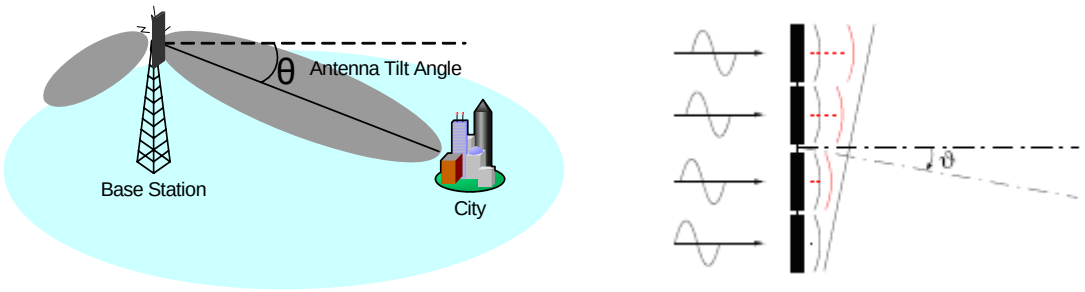

(a) *(b)*

Figure 21. Electrical tilt [Sio]

In earlier work, network implications due to electrical antenna downtilt [Nie1 and Iso] and mechanical antenna downtilt [Nie1 and Nie2] have been investigated. In [Nie1], capacity gain by means of electrical downtilt optimization was shown to be up to 48.4% with respect to the performance at 0˚ tilt in a scenario with 1.5 km ISD. As discussed in [Nie1 and Nie2] mechanical antenna downtilt also improves network capacity, in the same initial network conditions, providing a gain of 45.6%.

4.3. Modeling of Antenna Parameters

4.3.1. Antenna Radiation Pattern

In LTE simulations, the two equations below are applied to model horizontal and vertical radiation patterns [TR36.814]:

$$A_H(\varphi) = -\min\left[12\left(\frac{\varphi}{\varphi_{3dB}}\right), A_m\right], \; A_m = 25dB \tag{10}$$

$$A_V(\theta) = -\min\left[12\left(\frac{\theta}{\theta_{3dB}}\right), SLA_v\right], \; SLA_v = 20dB \tag{11}$$

It needs to be considered that antenna characteristics, e.g., the patterns which are shown in Figures 22 and 23 [Pow], are typically measured in an anechoic chamber, whereas in real-world deployment there are the significant impacts of scattering in the near field of the antenna (e.g., mast, mountings, other objects in the vicinity, such as roof-top, etc.) and diffraction. These near-field scatterers and diffractions are not accounted for by the propagation models; therefore, they need to be conceptually included in an effective antenna pattern. A basic property of such an effective antenna pattern would be the attenuation of

nulls, reduction in the front-to-back attenuation A_m and the side lobe attenuation SLA_v as shown in Figures 22 and 23 respectively. It is also visible that the design of the narrow vertical beam in a practical antenna leads to more severe and strong side lobes than we encountered in case of a wider horizontal pattern.

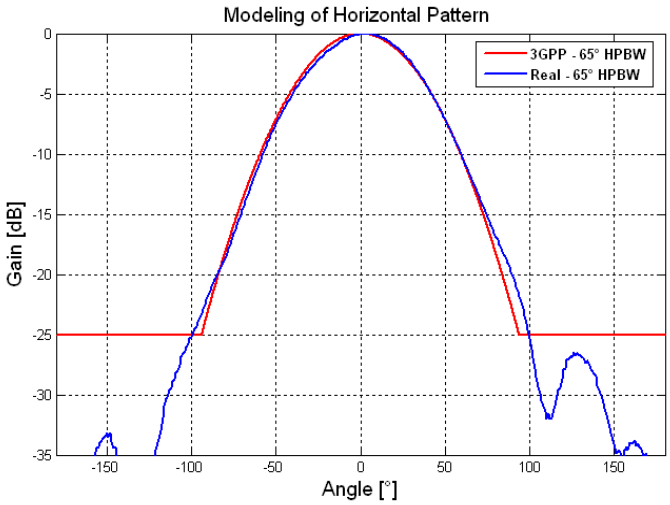

Figure 22. Modeling of horizontal pattern

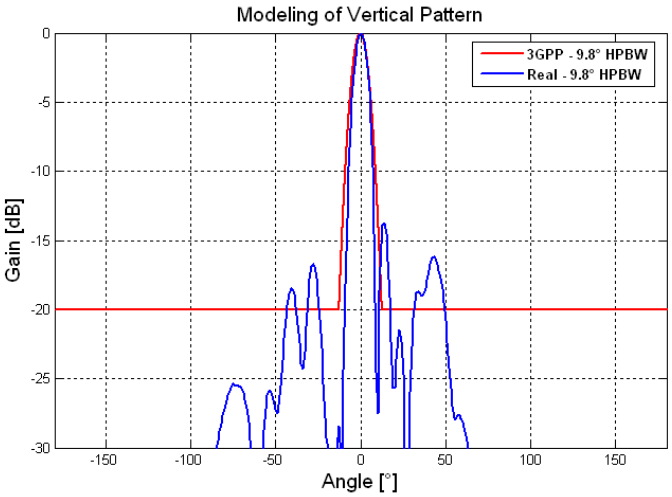

Figure 23. Modeling of vertical pattern

Extrapolation of the three dimensional (3D) pattern from two perpendicular cross-sections, azimuth and elevation patterns, is defined in [TR36.814] as shown below:

$$A(\varphi,\theta) = -\min\{-[A_H(\varphi) + A_V(\theta)], A_m\} \quad (12)$$

In the model applied for the simulations, the antenna characteristics are combined as a sum of antenna gain, horizontal pattern and elevation pattern. The sum of horizontal and vertical patterns is limited for a common front-to-back attenuation A_m because it takes into account the inaccuracies of real-world implementations and corresponds better to the limited isolations of co-sited sectors typically found in field measurements.

4.3.2. Modeling of Electrical and Mechanical Tilt

In electrical downtilt, main, side and back lobes are tilted uniformly by adjusting phases of antenna elements [Lee]. However, in mechanical downtilt, antenna main lobe is lowered on one side and the antenna back lobe is raised on the other side because antenna elements are physically directed towards ground [Sio]. Since mechanical downtilt has an impact on the radiation pattern in three dimensions, the horizontal offset angle is also included in the equation to calculate the effective downtilt angle [TR36.814] as shown in (13):

$$\zeta(i,k) = \arctan(\cos\theta(i,k)\tan\delta(i)) \tag{13}$$

where $\zeta(i,k)$ is the corresponding (electrical) downtilt angle for mobile user k which is served or interfered by cell i in radians with the mechanical downtilt angle $\delta(i)$ in radians, and the horizontal offset angle $\theta(i,k)$ in radians.

The angle $\phi(i,k)$ between the main lobe center and line connecting cell i and mobile terminal k in radians in the vertical plane $\phi(i,k)$ can be obtained by the following equations (14 and 15) [TR36.814]:

$$\omega(i,k) = \arctan\left(\frac{h(i)}{d(i,k)}\right) \tag{14}$$

$$\phi(i,k) = \omega(i,k) - \varphi(i) \tag{15}$$

where $d(i,k)$ is the distance between mobile user k and cell i, $h(i,k)$ is the height difference between the antenna of mobile user k and the antenna of cell i, $\omega(i,k)$ is the antenna-mobile line-of-sight angle in radians, and $\varphi(i)$ is the electrical downtilt angle of cell i in radians.

4.3.3. Modeling of Vertical Sectorization

In 3x2 vertical sectorization modeling, the transmission power of a cell in 3-sector layout is shared between two vertical sectors as defined in (16). In simulation studies, equal power is given for each vertical sector as shown in Figure 24.

$$P_{total} = P_{inner} + P_{outer} \tag{16}$$

where P_{total} is the total transmission power per conventional sector and P_{inner}, P_{outer} are the transmission powers of inner and outer vertical sectors respectively.

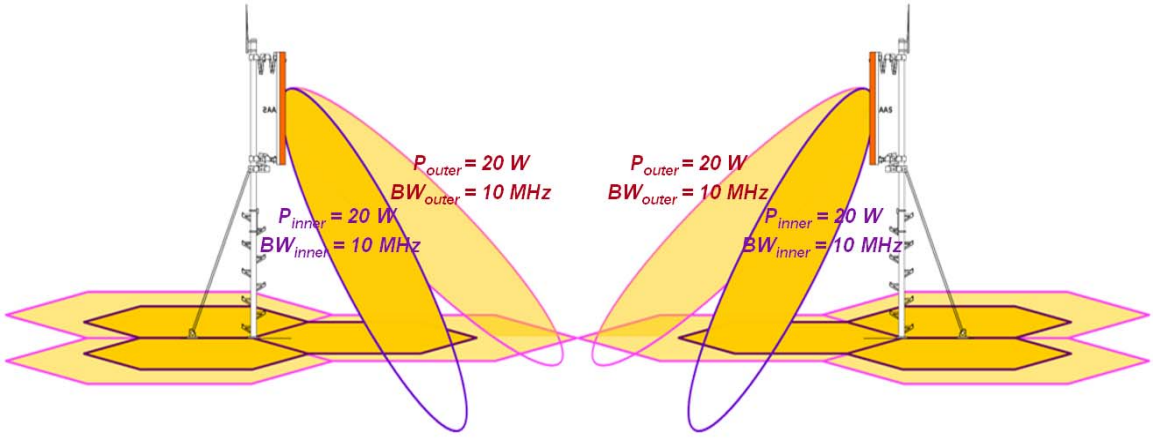

Figure 24. System bandwidth and transmission power in 3x2 vertical sectorization

The same system bandwidth is used for both sectors as shown in Figure 24 and defined in (17) so that the amount of resources are doubled but the power per PRB is halved.

$$BW_{system} = BW_{inner} = BW_{outer} \tag{17}$$

where BW_{system} is the system bandwidth and BW_{inner}, BW_{outer} denote the bandwidths of inner and outer vertical sectors respectively.

5. SIMULATION RESULTS

5.1. Analysis of Antenna Parameter Optimization Space

Simulations are carried out for the scenarios, 3GPP case 1 and case 3, based on the main simulation assumptions [TR25.814 and TR36.814] as defined in Appendix B. Optimization space for the parameters given in Table 2 is analyzed in this section.

Table 2. Simulation assumptions - Analysis of Antenna Parameter Optimization Space

Parameter	**Value**
Horizontal HPBW	$\varphi_{3dB} = 45^o, 55^o, 65^o, 70^o, 75^o, 85^o$
Vertical HPBW	$\theta_{3dB} = 4.4^o, 6.8^o, 9.4^o, 10^o, 13.5^o$
RET range	$\theta_{\text{etiltrange}} = \left[0^o \quad 20^o\right]$

In 3GPP case 1, it is observed that wider horizontal beam patterns and larger downtilt angles provide better coverage and capacity performance as inter-cell interference is dominant. When the half-power beamwidth of the horizontal pattern is altered, variation in the optimal downtilt is not remarkable as shown in Figure 25. Thus, the optimum tilt angle does not depend too much on the selected horizontal HPBW in 3GPP case 1.

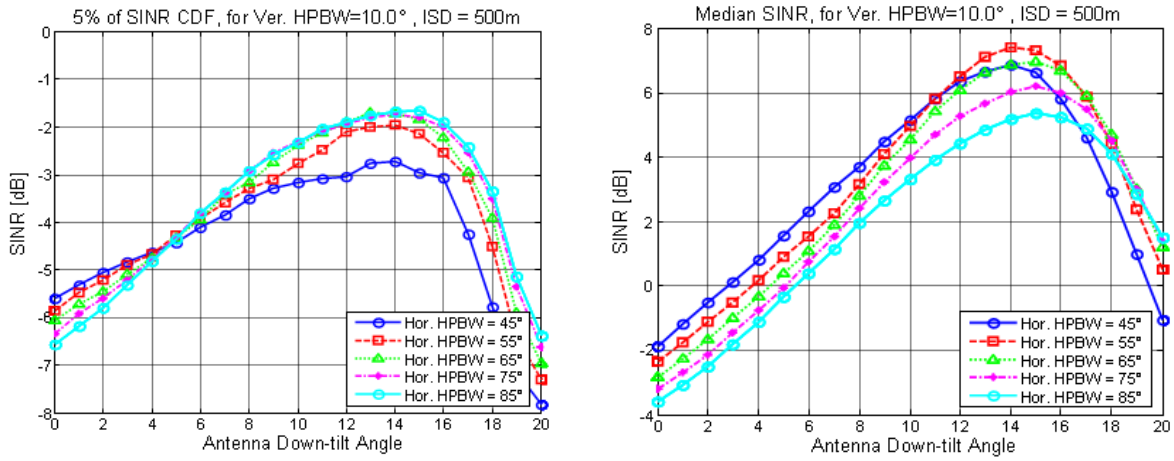

(a) *(b)*

Figure 25. Horizontal HPBW vs. coverage (a) and capacity (b) in 3GPP Case 1

In the noise-limited sparse network scenario (3GPP case 3), the impact of the horizontal half-power beamwidth and downtilt angle at the cell-edge is not significant, whereas the combination of smaller horizontal HPBW and moderate downtilt angle gives the network a notable performance gain in terms of capacity as shown in Figure 26.b.

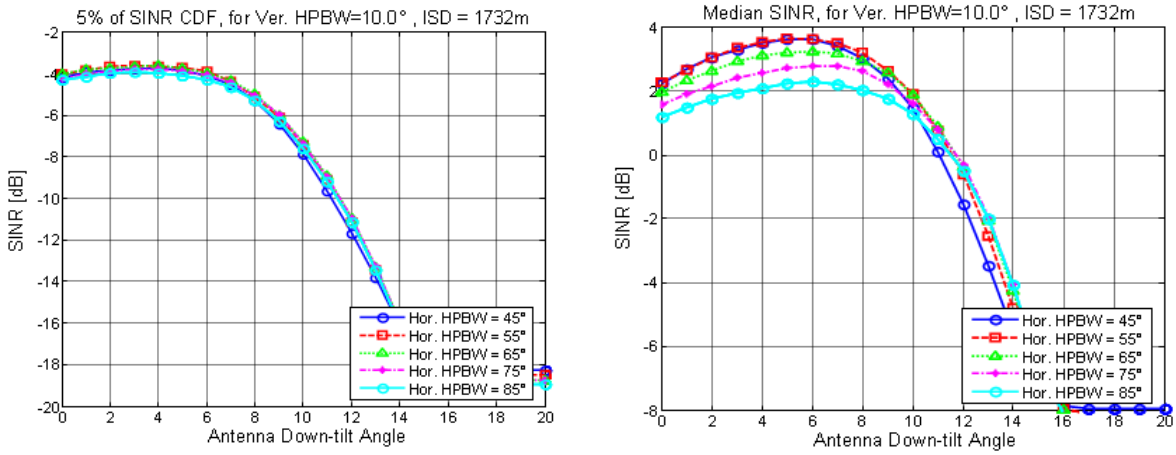

(a) *(b)*

Figure 26. Horizontal HPBW vs. coverage (a) and capacity (b) in 3GPP Case 3

As shown in Figure 27, the optimal downtilt angle in 3GPP case 1 varies with the selected vertical HPBW unlike the horizontal HPBW. Since antennas are not perfect in practice, the systems that have bigger vertical HPBWs should be selected in interference limited dense networks to be more robust against implementation errors.

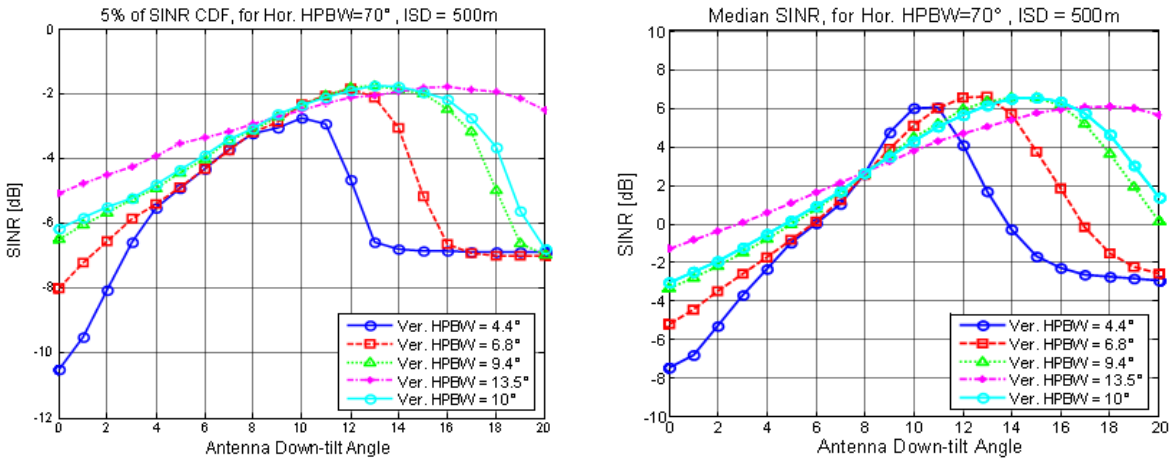

(a) *(b)*

Figure 27. Vertical HPBW vs. coverage (a) and capacity (b) performance in 3GPP Case1

In 3GPP case 3, narrower vertical beam patterns and moderate electrical downtilt angles provide remarkable gain in terms of both coverage and capacity as observed from Figure 28. On the other hand, tilt optimization is still not as effective as in 3GPP case 1 even with smaller HPBWs due to the fact that the noise limits the SINR rather than interference. Here, it should be also pointed out that optimum downtilt angles for smaller vertical HPBWs (e.g., 4.4˚) can provide higher gain especially for the capacity in 3GPP case 3 but erroneous

downtilt angle easily leads to a greater decrease in SINR than in the case of a larger vertical beam pattern.

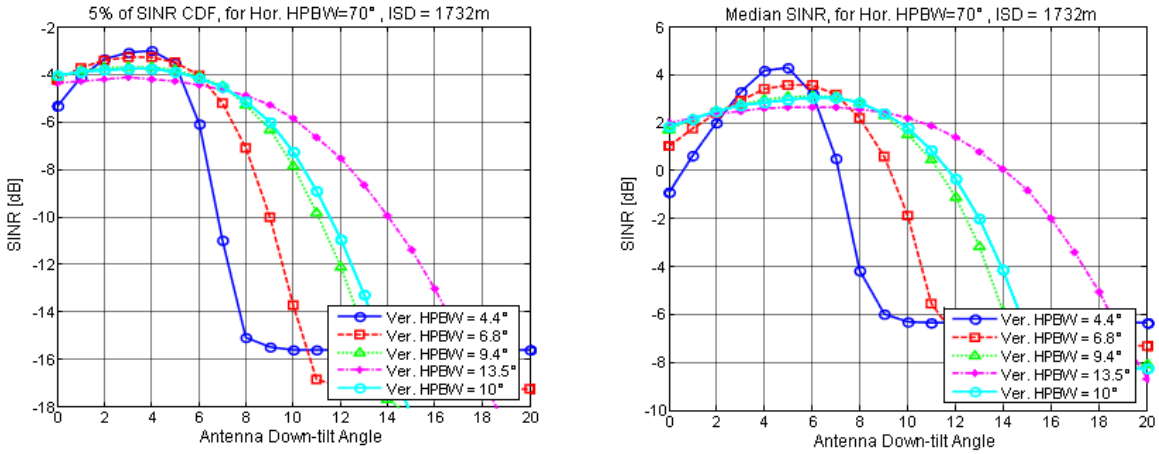

(a) *(b)*

Figure 28. Vertical HPBW vs. coverage (a) and capacity performance (b) in 3GPP Case3

The gains obtained from HPBW and downtilt optimizations might be different in synthetic test networks with uniform inter-site distances than they would be in practical networks where inter-site distances and antenna elevations vary from site to site. Yet, gains in practical networks are always case dependent; therefore, investigation of synthetic 3GPP test cases is justified. It should be noted that a self-optimization of beam patterns and remote electrical tilt is needed to reach similar coverage and capacity performance in practical networks.

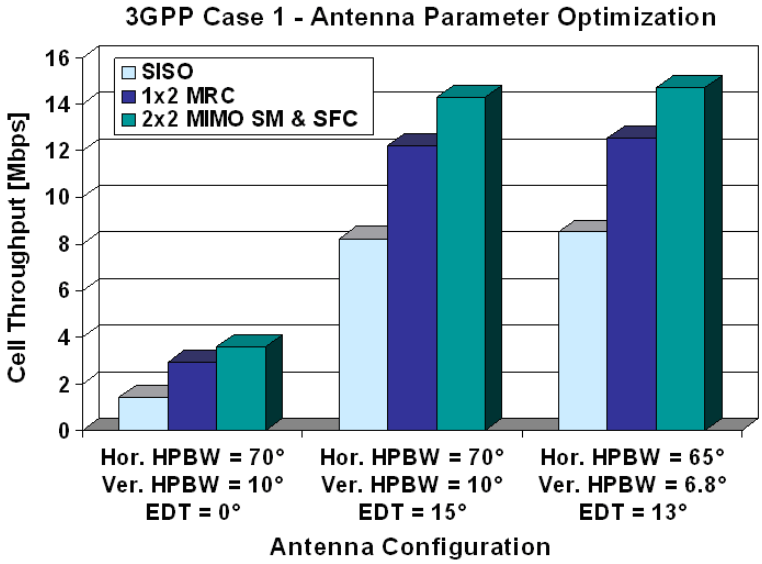

Figure 29. Throughput evaluation for 3GPP Case 1

When the cell throughput is analyzed for the antenna configurations with the optimum downtilt angles but the default HPBWs specified in [TR36.814] and the antenna configurations with optimal tilt, horizontal and vertical HPBWs; it is observed that antenna tilt parameter has a major impact on the network performance especially for 3GPP case 1 as shown in Figure 29. On the other hand, 3GPP case 3 is more robust against wrong downtilt angles, and narrower antenna beam patterns may provide higher capacity for larger inter-site distances as observed from Figure 30.

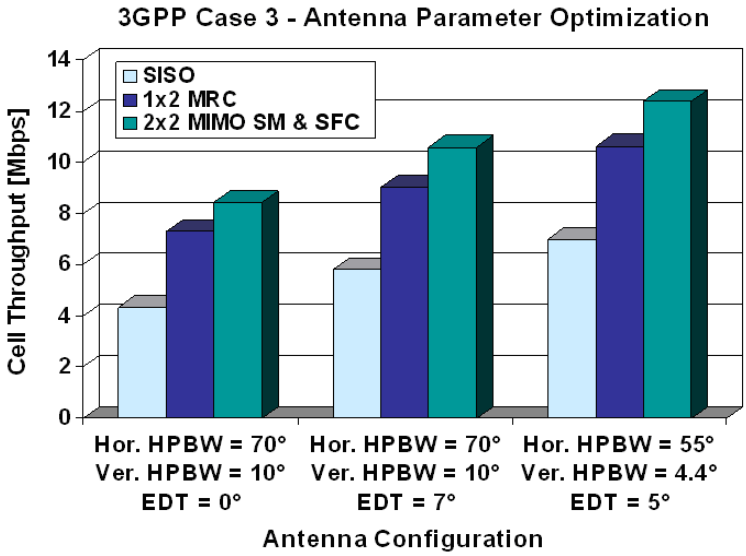

Figure 30. Throughput evaluation for 3GPP Case 3

5.2. Comparison of Electrical and Mechanical Antenna Downtilt Optimizations

Simulations are carried out for the scenarios, 3GPP case 1 and case 3, based on the main simulation assumptions [TR25.814 and TR36.814] as defined in Appendix B and the tilt ranges given in Table 3.

Table 3. Simulation assumptions - Comparison of EDT and MDT Optimizations

Parameter	**Value**
MDT range	$\theta_{\text{mtiltrange}} = [0^{o} \quad 20^{o}]$
EDT range	$\theta_{\text{etiltrange}} = [0^{o} \quad 20^{o}]$

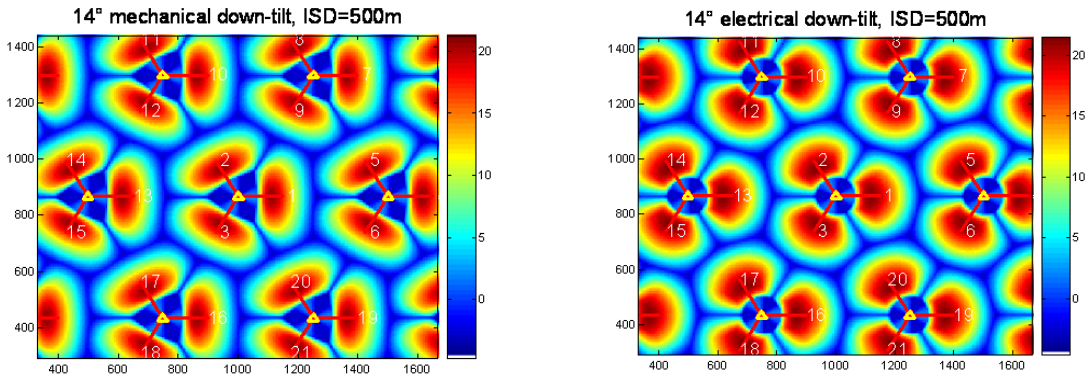

(a) *(b)*

Figure 31. Mechanical (a) vs. Electrical(b) DT in 3GPP case 1 for 0 dB shadowing

The optimizations of electrical and mechanical downtilt techniques are mainly discussed in this section. Figure 31 illustrates the difference between mechanical and electrical downtilt in terms of SINR for 3GPP case 1. To emphasize the difference shadow fading is set to 0 dB. Figure 31 also reflects the fact that antenna gain pattern keeps its original shape well in the case of electrical downtilt, whereas the shape of the antenna gain pattern may admit remarkable change when the mechanical downtilt is applied. On the other hand, since electrical tilt range is limited in practice due to changing side-lobe level, the impact of the hybrid approach which includes both mechanical and electrical downtilts with different proportions is investigated to find an optimal solution in terms of network performance.

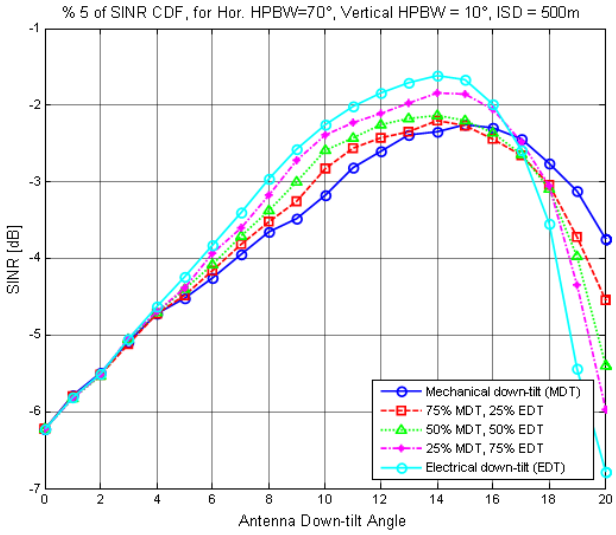

Figure 32. Coverage performance of mechanical and electrical downtilt for 3GPP case 1

In interference limited dense networks, where ISD is 500 m, the electrical downtilt provides better performance both in terms of coverage and capacity as shown in Figures 32 and 33. In this case electrical downtilt can offer around 1 dB better SINR performance with respect to mechanical downtilt.

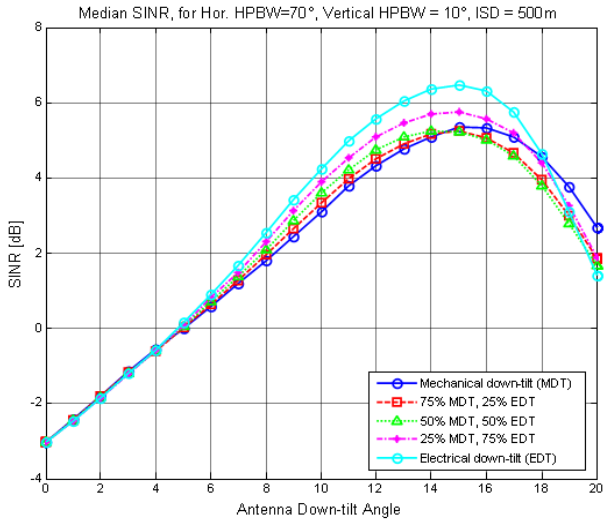

Figure 33. Capacity performance of mechanical and electrical downtilt for 3GPP case 1

The performance of mechanical and electrical tilts differs significantly from each other in 3GPP case 1 as observed from Figures 32 and 33 when using optimal tilt angles. According to Figure 34, throughput penalty due to the limited electrical tilt range might be large.

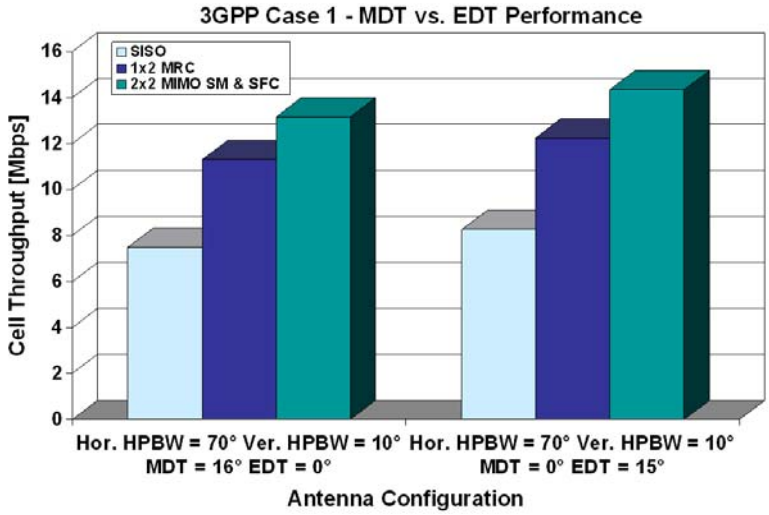

Figure 34. Cell throughputs in 3GPP case 1

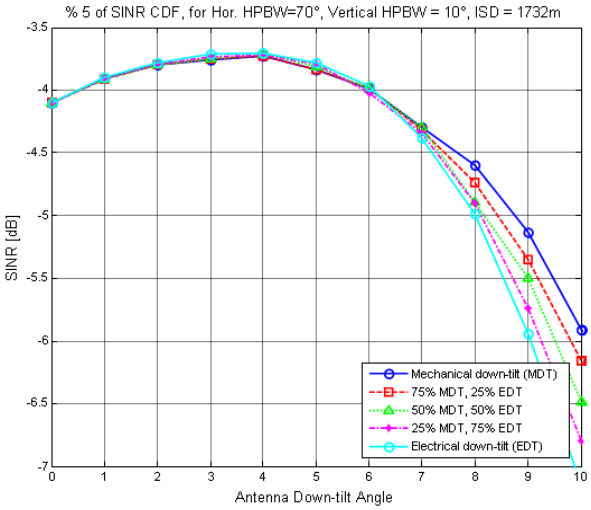

Figure 35. Coverage performance of mechanical and electrical downtilt for 3GPP case 3

In 3GPP case 3, neither electrical downtilt nor mechanical downtilt brings any significant gain in terms of coverage as shown in Figure 35. On the other hand, in capacity, it is still possible to provide notable gain by using either mechanical downtilt or electrical downtilt as observed from Figures 36 and 37 as mechanical and electrical downtilt techniques perform similarly in smaller downtilt angles.

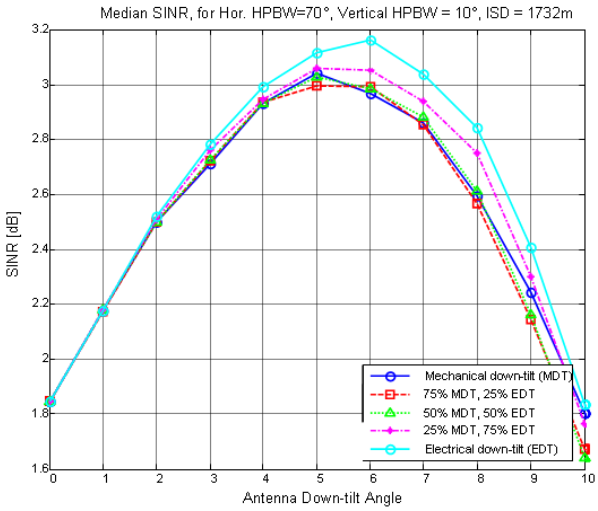

Figure 36. Capacity performance of mechanical and electrical downtilt for 3GPP case 3

In the case of long inter-site distances as in 3GPP Case 3, when the system becomes noise limited, the impact of electrical or mechanical downtilt is insignificant in terms of cell throughput as shown in Figure 37.

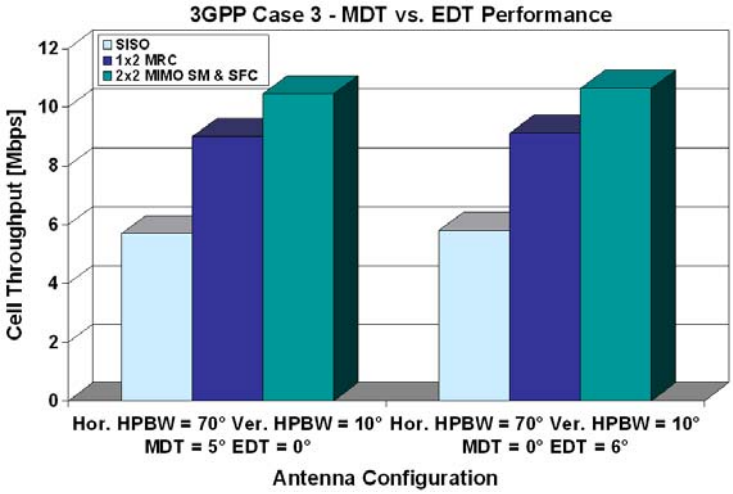

Figure 37. Cell throughputs in 3GPP case 3

5.3. Analysis of Vertical Sectorization

Simulations are carried out for the scenarios, 3GPP case 1 and case 3, based on the main simulation assumptions [TR25.814 and TR36.814] as defined in Appendix B and the modified assumptions given in Table 4.

Table 4. Simulation assumptions - Analysis of Vertical Sectorization

Parameter	**Value**
TX power	46 dBm (43 dBm/vertical sector)
Horizontal HPBW	$\varphi_{3dB} = 65^{o}$
Vertical HPBW	$\theta_{3dB} = 3.0^{o}, 4.4^{o}, 6.8^{o}$
RET range	$\theta_{\text{etiltrange}} = \left[0^{o} \quad 20^{o}\right]$

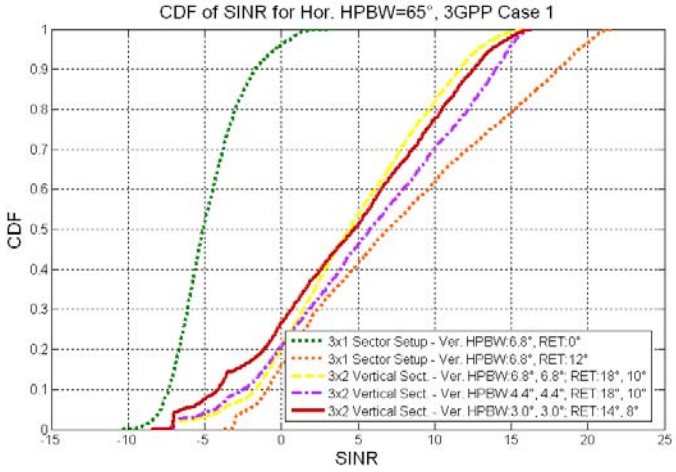

Figure 38. 3-Sector eNB vs. 3x2 Vertical sectorization in 3GPP Case 1

As seen from Figures 38 and 39, in both 3GPP case 1 and case 3, reduced power per PRB and additional interference from the adjacent vertical sector makes SINR worse for 3x2 vertical sectorization compared to the standard 3-sectorized setup.

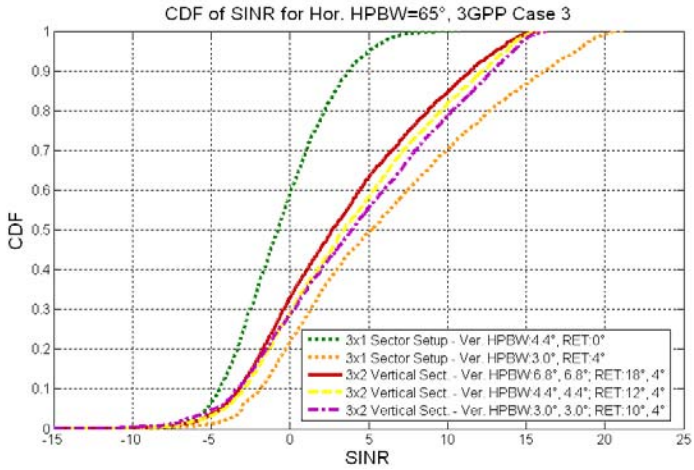

Figure 39. 3-Sector eNB vs. 3x2 Vertical sectorization in 3GPP Case 3

Antenna downtilt and vertical HPBW parameters that provide optimal performance are selected for the detailed capacity and throughput evaluations. In Figure 40, maximum achievable capacity gains for the cells in the 3-sector layout and the vertical sector pairs in the 3x2 vertical sectorization setup are compared. Although there is a remarkable decrease in SINR in both simulation scenarios, since the same resources can be used in both sectors, overall performance improves.

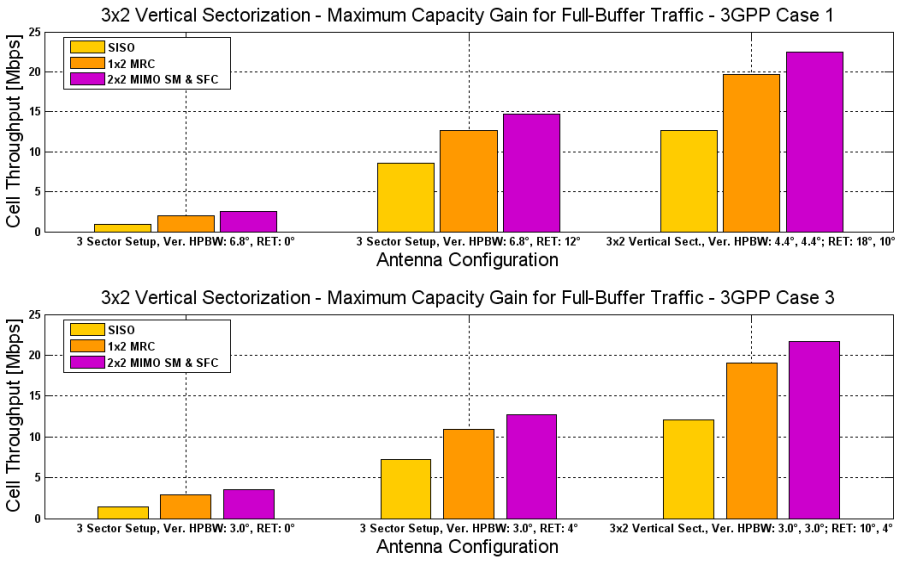

Figure 40. Maximum capacity gain for 3x1 and 3x2 sector layouts in 3GPP case 1 and case 3

As it can be observed from the cell selection maps of the 3x2 vertical sectorized setup with optimized configurations (Figure 40) for 3GPP Case 1 and Case 3 in Figures 41 and 42 respectively, the outer vertical sector serves more users with respect to the inner vertical sector in the case of uniform user distribution (i.e., outer sector's load is 74% in 3GPP case 1 and 90% in 3GPP case 3).

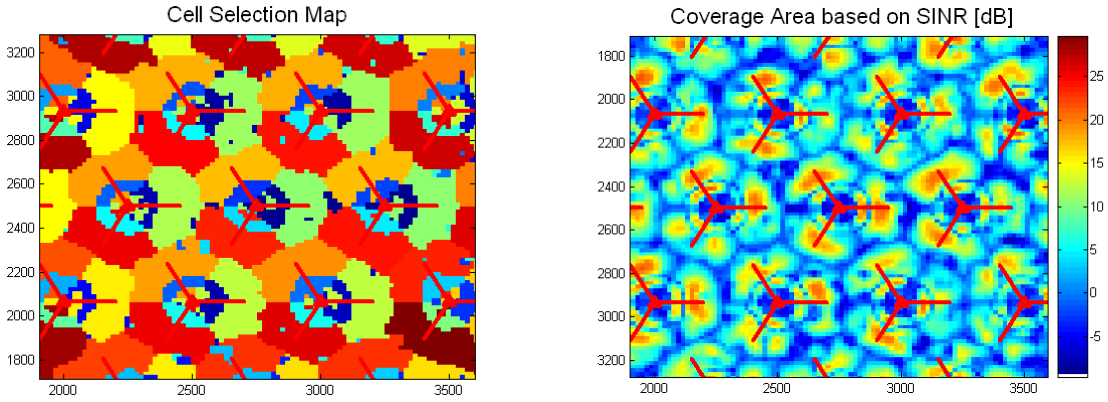

(a) *(b)*

Figure 41. Cell selection (a) and coverage (b) maps for 3GPP Case 1

Even though the vertical sectorization maximizes the overall cell capacity as shown in Figure 40; the impact of vertical sectorization on the user throughput depends on the load of each vertical sector. For instance, if the vertical HPBWs are 4.4˚, 4.4˚; and tilts are 18˚, 10˚ for inner and outer sectors respectively, the inner vertical sector has 44% of the available capacity of the vertical sector pair, while 26% of the users are served by the inner sector for uniform user distribution in 3GPP case 1. Moreover, the load imbalance between adjacent vertical sectors becomes more severe when the inter-site distance is larger.

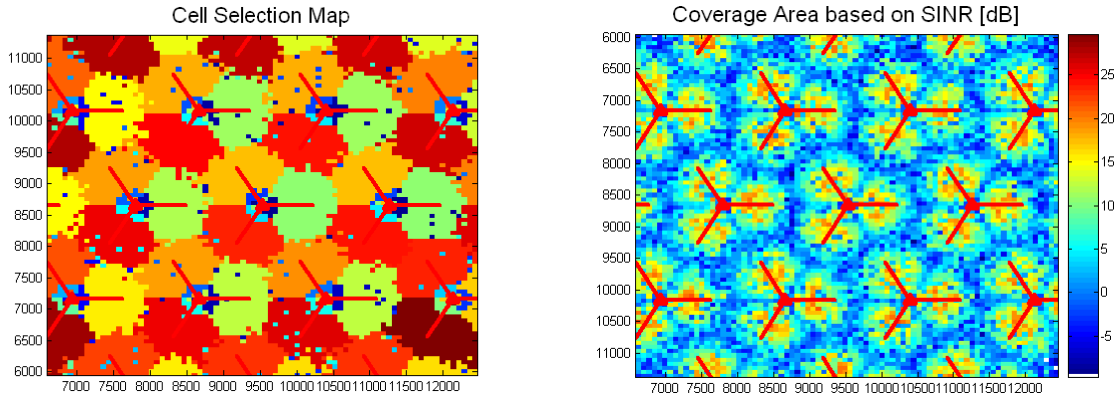

(a) *(b)*

Figure 42. Cell selection (a) and coverage (b) maps for 3GPP Case 3

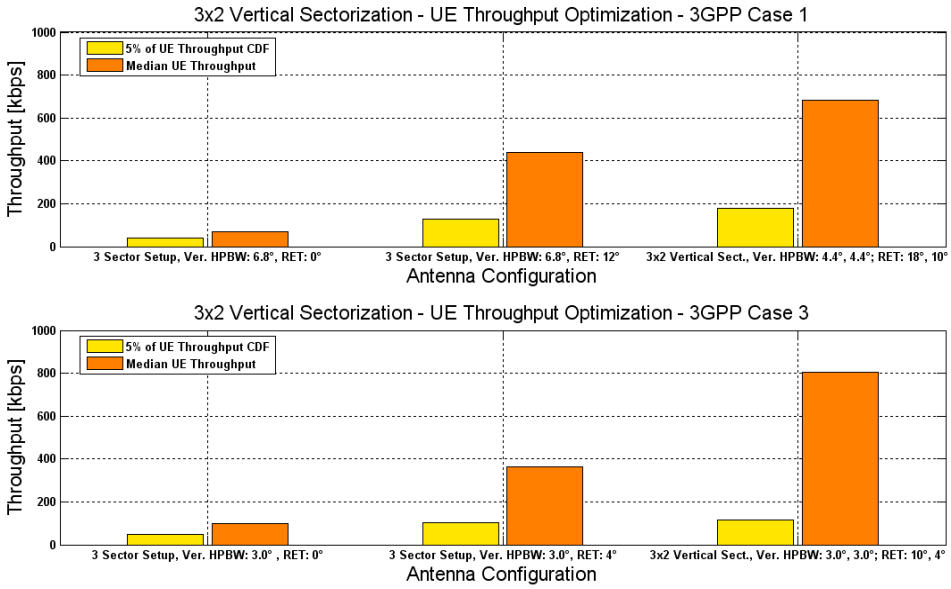

Figure 43. UE throughput optimization for 3x1 and 3x2 sector layouts in 3GPP Case 1 and Case 3

The vertical sectorization increases the number of satisfied users significantly as shown in Figure 43 in terms of median user throughput. On the other hand, the same amount of gain cannot be achieved for the cell edge UEs especially in 3GPP case 3.

5.4. Self-optimization of RET

Simulations for the self-optimization of remote electrical tilt is carried out in the irregular network layout of Helsinki downtown following the main simulation assumptions [TR25.814 and TR36.814] as defined in Appendix B and the modified assumptions given in Table 5.

Table 5. Simulation assumptions - Self-optimization of RET

Parameter	**Value**
Monitored cells in irregular network layout	2, 3, 4, 5, 6, 9, 10, 11, 14, 15, 16, 17, 18, 19, 20, 22, 23, 24, 25, 30, 32
RET range	0˚ – 10˚
Horizontal HPBW	65˚
Vertical HPBW	8.5˚
Traffic model	Best-effort/CBR

To present fair assessment on the self-optimization of coverage and capacity, network edge cells, which are not affected by sufficient inter-cell interference, are left out from the evaluation.

As shown in Figure 44, most of the cells in the monitored area of the network are downtilted because the initial tilt angles are planned considering soft handover (SHO) gain for the WCDMA network. On the other hand, hard handover (HHO) is used for LTE instead. That is one of the main reasons why tilt angles are increased and cell overlapping area gets smaller after the self-optimization of remote electrical tilt.

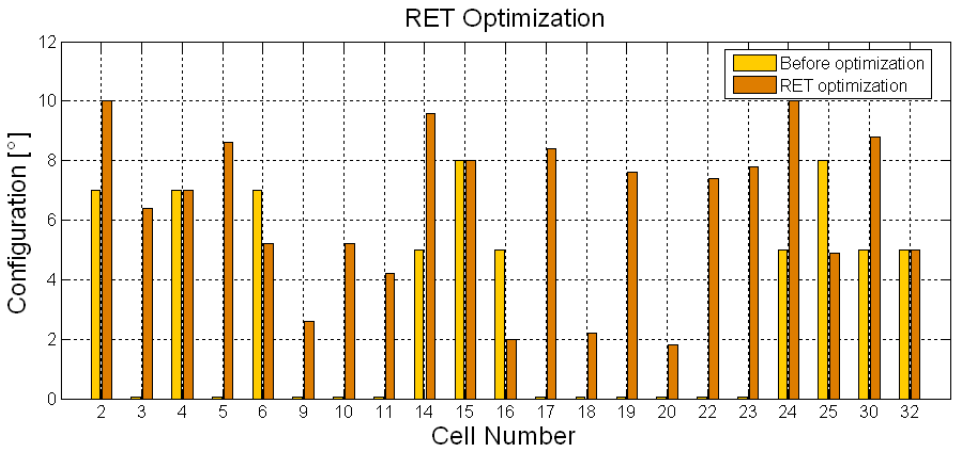

Figure 44. Configuration of RET before and after optimization

The performances of SINR and user throughput, shown in Figures 45 and 46 respectively, are slightly different than each other due to varying load in the cells and nonlinear correlation between SINR and throughput. The 5%-ile (a) and 50%-ile (b) of the cumulative distributions of SINR and user throughput justify that optimization is achieved despite the small number of fluctuations that occur due to the cells which are already close to their optimal performance level.

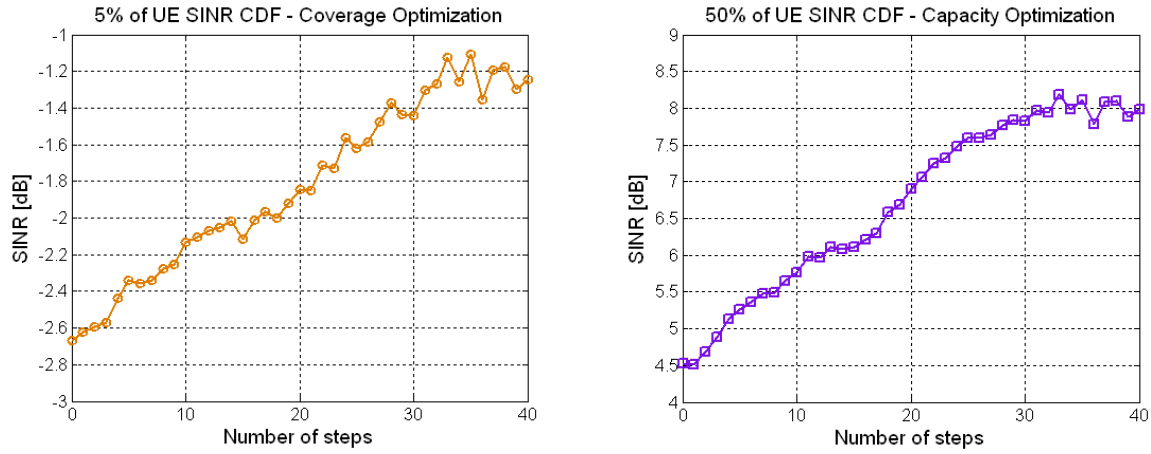

(a) *(b)*

Figure 45. Optimization of SINR in best-effort traffic model

As shown in Figure 46, it is possible to achieve 16% and 46% throughput improvements for the UEs located at the cell-edge and the cell-center respectively. It also justifies the previous studies related to antenna parameter optimization space and remote electrical tilt performance since more significant gains are also observed in the capacity performance rather than coverage in [Yil1 and Yil2].

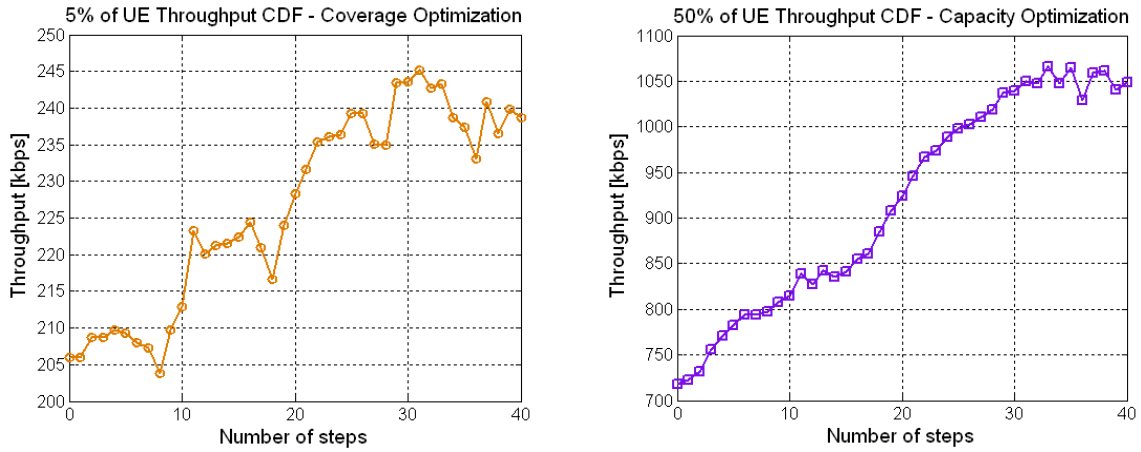

(a) *(b)*

Figure 46. Optimization of UE throughput in best-effort traffic model

Cell capacities are improved about 23% on average after self-optimization. On the other hand, the level of capacity gain differs from cell to cell due to varying traffic and propagation conditions. It should be also noted that capacity optimization is observed even for the cells where antenna tilts are not changed by means of the decreased inter-cell interference.

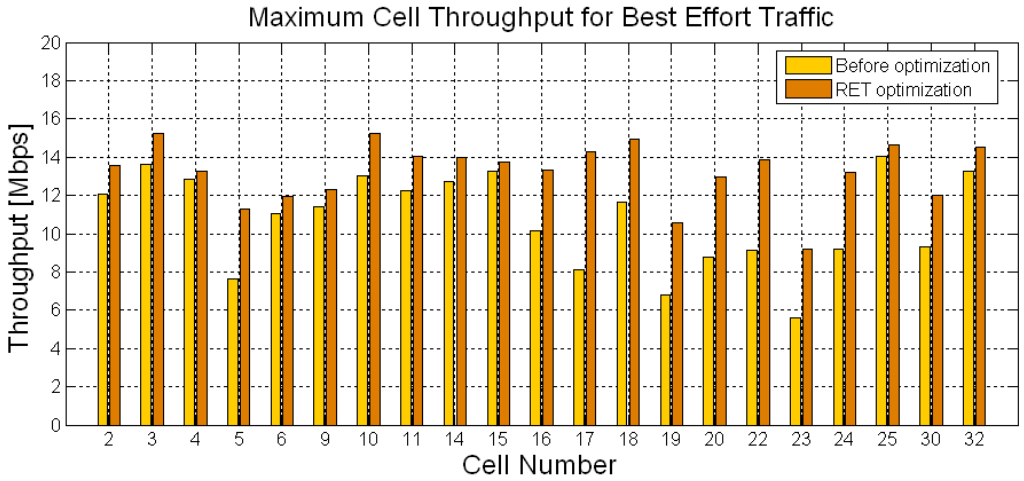

Figure 47. Optimization of cell throughput in best-effort traffic model

The average achievable Guaranteed Bit Rate (GBR) is calculated to evaluate Constant Bit Rate (CBR) traffic performance assuming all UEs are served with maximum achievable GBR. As observed from Figure 47, RET optimization also improves the performance in the CBR traffic scenario.

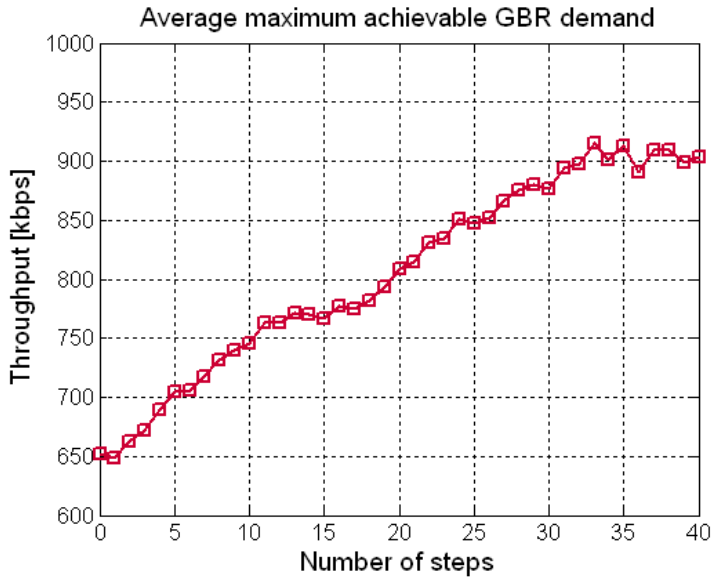

Figure 48. UE throughput optimization for CBR traffic

5.5. Self-optimization of Antenna Azimuth and Horizontal HPBW

Simulations for the self-optimization of antenna azimuth and horizontal HPBW are carried out in the irregular network layout of Helsinki downtown with non-optimized antenna parameters. The main simulation assumptions of LTE and LTE-A technologies [TR25.814 and TR36.814] that are described in Appendix B and the modified assumptions given in Table 6 are followed by the system level simulator.

Table 6. Simulation assumptions - Self-optimization of Antenna Azimuth and HPBW

Parameter	**Value**
Monitored cells in irregular network layout	2, 3, 4, 5, 6, 9, 10, 11, 14, 15, 16, 17, 18, 19, 20, 22, 23, 24, 25, 30, 32
Horizontal HPBW selection	65˚ (default), 35˚ – 125˚ (step size: 10˚)
Vertical HPBW	8.5˚
Horizontal beam steering selection	0˚ (default), -40˚ – 40˚ (step size: 10˚)
Antenna technique	1x2 MRC
Traffic model	Best-effort/CBR

Optimizations of the antenna azimuth and horizontal HPBW may be other attractive solutions that can be applied for the coverage and capacity optimization use case following the algorithm structure which is proposed in Chapter 3.

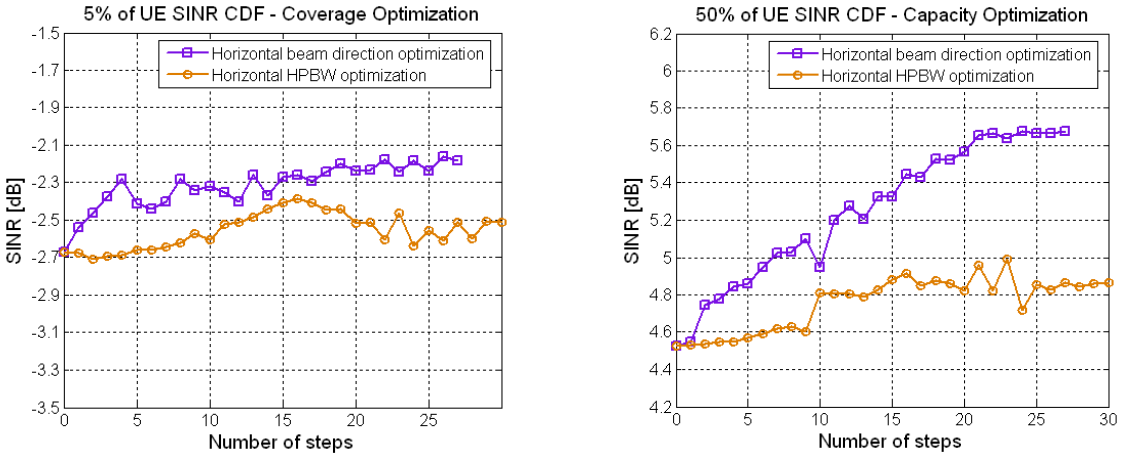

(a) *(b)*

Figure 49. SINR optimization for monitored cells

Antenna azimuth optimization provides notable gain in terms of both capacity and coverage as shown in Figures 49 and 50. The improvement, however, in the network performance is smaller with respect to the level of optimization achieved by self-optimization of RET. The third parameter of antenna parameter optimization which is horizontal HPBW does not bring significant capacity gain into the system. What is more, it indicates a danger in the coverage performance of best-effort traffic users as it changes not only the antenna gain but also the shape of horizontal beam pattern.

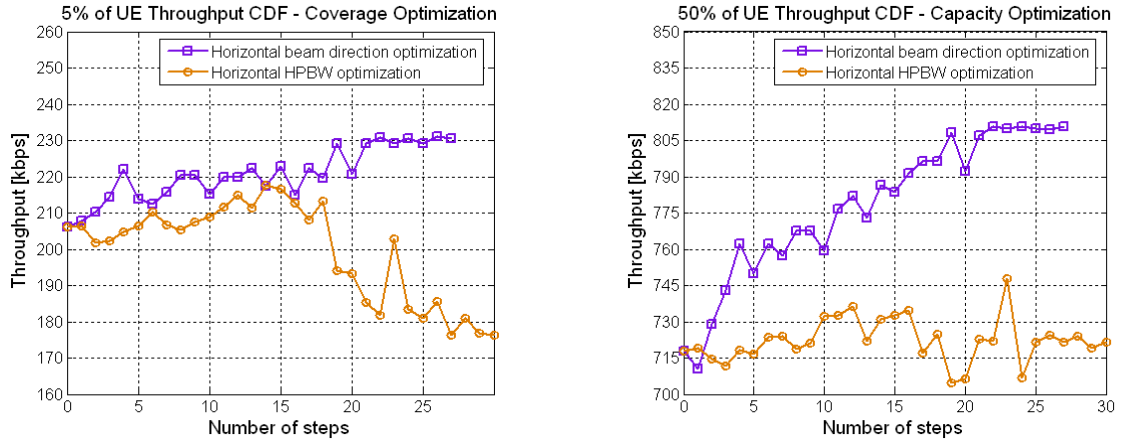

(a) *(b)*

Figure 50. Best-effort UE throughput optimization for monitored cells

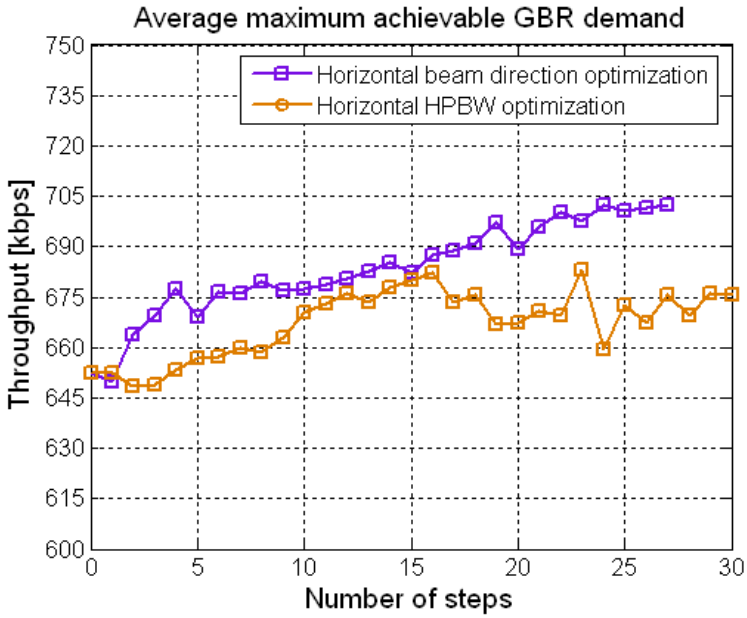

Figure 51. GBR UE throughput optimization for monitored cells

The average achievable GBR is used as an indicator for the evaluation of CBR traffic performance following the same calculation approach applied in the self-optimization of RET. As observed from Figure 51, only the optimization of horizontal beam direction improves the UE throughput performance consistently in the case of CBR traffic.

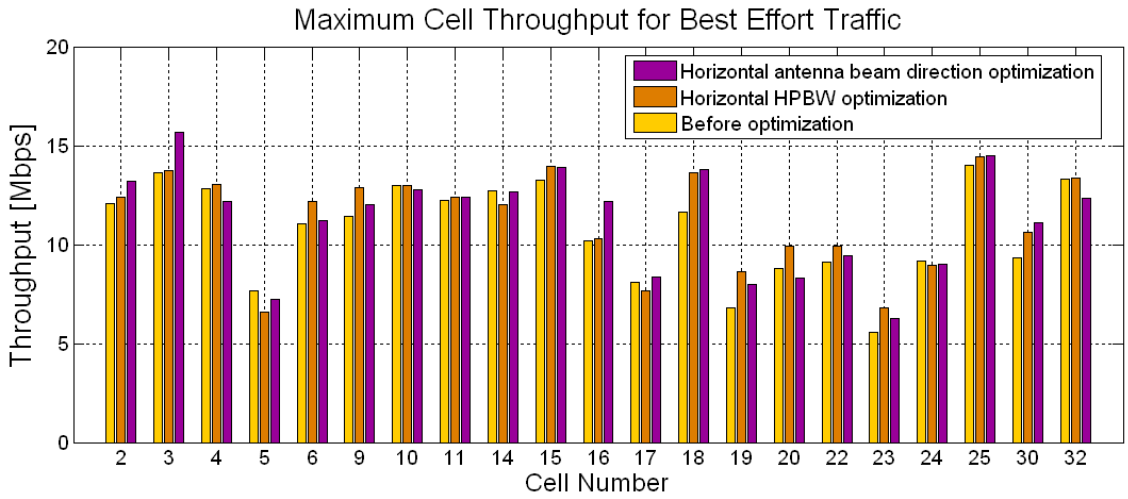

Figure 52. Best-effort cell throughput optimization for monitored cells

The self-optimization of antenna azimuth helps most of the cells maximize their capacities. On the other hand, it cannot be guaranteed that all cell performance will be improved after

the self-optimization as the goal of the self-optimization is to provide overall optimization in the network performance as justified by the simulation results in Figures 51 and 52.

6. CONCLUSIONS AND FUTURE WORK

The thesis work investigated the self-optimization of coverage and capacity in LTE networks using adaptive antenna systems. In the thesis, simulations on the optimization space of antenna parameters and the comparison of mechanical and electrical tilt optimizations yielded the necessary insights for the development of self-optimization algorithms. Furthermore, the vertical sectorization as a novel AAS technology was discussed aiming to build a future self-optimization use case.

In simulation results, it is observed that the antenna tilt parameter has the major impact on the network performance especially in the interference limited conditions. Since there are two different types of antenna tilt techniques, system performance results in the presence of both mechanical and electrical tilt techniques were simulated as well. Simulation results showed that electrical downtilt performs much better in interference-limited dense networks, whereas the performance slightly differs from each other in noise-limited sparse networks. It is also worth noticing that coverage and capacity criteria may lead to different optimal tilt angles in dense urban networks.

In the thesis work, the impact of a novel AAS method that is called vertical sectorization on LTE network performance was analyzed. It is shown that vertical sectorization may be an important mean to achieve IMT-A targets if vertical sectorization parameters can be dynamically optimized based on the load conditions in inner and outer vertical sectors.

Finally, the thesis focused on the coverage and capacity optimization use case by means of the adaptive adjustment of RET, antenna direction and horizontal HPBW. It is shown that the self-optimization of antenna tilts and directions may provide significant performance improvements in instances of suboptimal network planning or reuse of 3G network planning, and/or varying radio network environment conditions.

Future work for the shown studies includes corresponding simulations in the uplink direction of LTE as well as base station transmit power optimization in the scope of the coverage and capacity optimization and interference reduction use cases. Moreover, other use cases such as

RACH optimization, mobility load balancing and mobility robustness optimization as well as self-coordination of those use cases will be future topics in the research area of SON.

REFERENCES

[3GPP] Overview of 3GPP Long Term Evolution, available at http://www.3gpp.org/LTE.

[Aha] D.W. Aha, “Case-Based Learning Algorithms”, In Proceedings of Case-Based Reasoning Workshop, pp.147–158, 1991.

[Bal] C.A. Balanis, *Antenna Theory*, John Wiley & Sons Inc., Revised Edition, 2005.

[Dot] M. Dottling and I. Viering, “Challenges in mobile network operation: Towards self-optimizing networks”, in Proceedings of IEEE International Conference on Acoustics, Speech and Signal Processing, Taipei, Taiwan, April 2009.

[Ell] R.S. Elliot, *Antenna Theory and Design*, John Wiley & Sons Inc., 3rd Edition, 2003.

[Fos] G.J. Foschini and M.J. Gans, “On limits of wireless communications in a fading environment when using multiple antennas”, Wireless Personal Communication, vol. 6, pp. 311-335, 1998.

[Fuj] K. Fujimoto and J.R. James, *Mobile Antenna Systems Handbook*, Artech House, Norwood, MA, 1994.

[Hol] H. Holma and A. Toskola, *LTE for UMTS OFDMA and SC-FDMA Based Radio Access*, John Wiley & Sons Ltd., 2009.

[Iso] T. Isotalo, J. Niemelä, and J. Lempiäinen, “Electrical antenna downtilt in UMTS network,” in Proceedings of European Wireless Conference, pp. 265–271, Barcelona, Spain, February 2004.

[Jen1] M.A. Jensen and Y. Rahmat-Samii, “Performance Analysis of Antennas for Hand-Held Transceivers Using FDTD”, IEEE Transactions on Antennas and Propagation, Vol. 42, No. 8, pp. 1106–1113, August 1994.

[Jen2] M.A. Jensen and Y. Rahmat-Samii, “EM Interaction of Handset Antennas and a Human in Personal Communications”, in Proceedings of the. IEEE, Vol. 83, No. 1, pp. 7–17, January 1995.

[Kat1] K.D. Katsibas, *Analysis and Design of Mobile Antennas for Handheld Units*, Master's thesis, Arizona State University, Arizona, USA, August 1996.

[Kat2] K.D. Katsibas, C.A. Balanis, P.A. Tirkas, and C.R. Birtcher, "Folded Loop Antenna for Mobile Handheld Units", IEEE Transactions on Antennas and Propagation, Vol. 46, No. 2, pp. 260–266, February 1998.

[Lai] J. Laiho, A. Wacker, and T. Novasad, *Radio Network Planning and Optimization for UMTS*, John Wiley & Sons Inc., 2nd Edition, 2006.

[Lan] P. Langley and W. Iba, "Average-Case Analysis of a Nearest Neighbor Algorithm", In Proceedings of the 13th IJCAI, pp.889–894, 1993.

[Lee] W.C.Y. Lee, *Mobile Communications Engineering*, McGraw-Hill, 1998.

[Les] P. Lescuyer and T. Lucidarme, *Evolved Packet System (EPS): the LTE and SAE Evolution of 3G UMTS*, John Wiley & Sons Ltd., 2008.

[Mog] P. Mogensen et al., "LTE Capacity compared to the Shannon Bound", IEEE Vehicular Technology Conference, Dublin, Ireland, May 2007.

[NGMN1] Next Generation Mobile Networks, "Use Cases related to Self Organising Network, Overall Description," Version 2.02, April 2007.

[NGMN2] Next Generation Mobile Networks, "Nokia Siemens Networks View on Self Organizing Networks (SON)", NGMN Workshop, Darmstadt, Germany, November 2007.

[Nie1] J. Niemelä, T. Isotalo, and J. Lempiäinen, "Optimum Antenna Downtilt Angles for Macrocellular WCDMA Network", EURASIP Journal on Wireless Communications and Networking, vol. 2005, no. 5, pp. 816–827, 2005.

[Nie2] J. Niemelä and J. Lempiäinen, "Impact of mechanical antenna downtilt on performance of WCDMA cellular network," in Proceedings of IEEE Vehicular Technology Conference, vol. 4, pp. 2091–2095, Milan, Italy, May 2004.

[Pol] P. R. Sai A and C. Furse, “System level analysis of noise and interference analysis for a MIMO system,” in Proceedings of the IEEE International Symposium on Antennas and Propagation and USNC/URSI National Radio Science Meeting, pp. 1–4, 2008.

[Pow] BS antenna products, available at http://www.powerwave.com/antennaproducts.asp.

[Poz] D.M. Pozar, *Microwave Engineering*, John Wiley & Sons Inc., 2nd Edition, 1998.

[Sio] I. Siomina, P. Värbrand, and D. Yuan, “Automated Optimization of Service Coverage and Base Station Antenna Configuration in UMTS Networks”, IEEE Wireless Communications, 2006, Vol. 13, No. 6, pp. 16-25.

[Soc] SOCRATES, “Self-optimisation and self-configuration in wireless networks”, European Research Project, available at http://www.fp7-socrates.eu.org.

[Tel] I.E. Telatar, “Capacity of multi-antenna Gaussian channels,” European Transactions on Telecommunications, Vol. 10, No.6, pp. 585-595, 1999.

[TR25.814] 3GPP, TR 25.814 V7.1.0, *Physical layer aspect for evolved Universal Terrestrial Radio Access (UTRA)*.

[TR25.9121] 3GPP, TR 25.9121, *LTE Feasibility Study*.

[TR25.913] 3GPP, TR 25.913 V7.0.0, *Requirements for Evolved UTRA (E-UTRA) and Evolved UTRAN (E-UTRAN)*.

[TR25.943] 3GPP, TR 25.943 V8.0.0, *Deployment Aspects*.

[TR36.814] 3GPP, TR 36.814 V0.4.1, *Evolved Universal Terrestrial Radio Access (E-UTRA); Further advancements for E-UTRA Physical layer aspects*.

[TR36.902] 3GPP, TR 36.902 V9.0.0, *Self-configuring and self-optimizing network use cases and solutions*.

[TR36.913] 3GPP, TR 36.913 V8.0.1, *Requirements for further advancements for Evolved Universal Terrestrial Radio Access (E-UTRA)*.

[TS32.101] 3GPP, TR 32.101 V8.4.0, *Telecommunication management; Principles and high level requirements*.

[TS32.500] 3GPP; TS 32.400 V8.0.0, *Telecommunication Management; Self-Organizing Networks (SON); Concepts and requirements*.

[TS36.104] 3GPP, TS 36.104 V8.3.0, *Evolved Universal Terrestrial Radio Access (E-UTRA); Base Station (BS) radio transmission and reception*.

[TS36.133] 3GPP, TS 36.133 V9.2.0, *Evolved Universal Terrestrial Radio Access (E-UTRA); Requirements for support of radio resource management*.

[TS36.211] 3GPP, TS 36.211 V9.0.0, *Evolved Universal Terrestrial Radio Access (E-UTRA); Physical Channels and Modulation*.

[TS36.213] 3GPP, TS 36.213 V8.7.0, *Evolved Universal Terrestrial Radio Access (E-UTRA); Physical layer procedures*.

[TS36.300] 3GPP, TS 36.300 V.9.0.0, *Evolved Universal Terrestrial Radio Access (E-UTRA) and Evolved Universal Terrestrial Radio Access Network (E-UTRAN); Overall Description, Stage 2*.

[Ueh] K. Uehara, “Random Case Analysis of Inductive Learning Algorithms”, In Proceedings of the First International Conference on Discovery Science, 1998.

[Vie] I. Viering, M. Dottling, and A. Lobinger, "A Mathematical Perspective of Self-Optimizing Wireless Networks," In Proceedingsof IEEE International Conference on Communications, vol., no., pp.1-6, June 2009

[Wei] N. Wei, et al., “Baseline E-UTRA Downlink Spectral Efficiency Evaluation,” IEEE Conf. on Vehicular Technology, 2006, Montreal, Canada.

[Wir] BS antenna products, available at http://wirelessconnect.eu.

[Yil1] O.N.C. Yilmaz, S. Hämäläinen, and J. Hämäläinen, “Analysis of Antenna Parameter Optimization Space for 3GPP LTE”, In Proceedings of IEEE Vehicular Technology Conference, Anchorage-Alaska, September 2009.

[Yil2] O.N.C. Yilmaz, S. Hämäläinen, and J. Hämäläinen, “Comparison of Remote Electrical and Mechanical Antenna Downtilt Performance for 3GPP LTE”, In Proceedings of IEEE Vehicular Technology Conference, Anchorage-Alaska, USA, September 2009.

[Yil3] O.N.C. Yilmaz, S. Hämäläinen, and J. Hämäläinen, “System Level Analysis of Vertical Sectorization for 3GPP LTE”, In Proceedings of IEEE International Symposium on Wireless Communication Systems, Siena-Tuscany, Italy, September 2009.

Appendix

A. Modeling of System Level Simulator

A static snap-shot system level LTE simulator is modeled for the antenna parameter optimization/self-optimization studies because of the fact that static simulators are much more convenient to run long-time optimization cycles even though dynamic simulators may provide more accurate results when impact of mobility is taken into account.

Propagation is modeled in three dimensions by adding to the impact of shadow fading and antenna configurations summing with the propagation loss values of each sector.

Throughput evaluations are performed using link to system level mapping where link-level simulation results [Mog] have been run assuming a 6-tap Typical Urban (TU) channel and a 10 km/h user mobility.

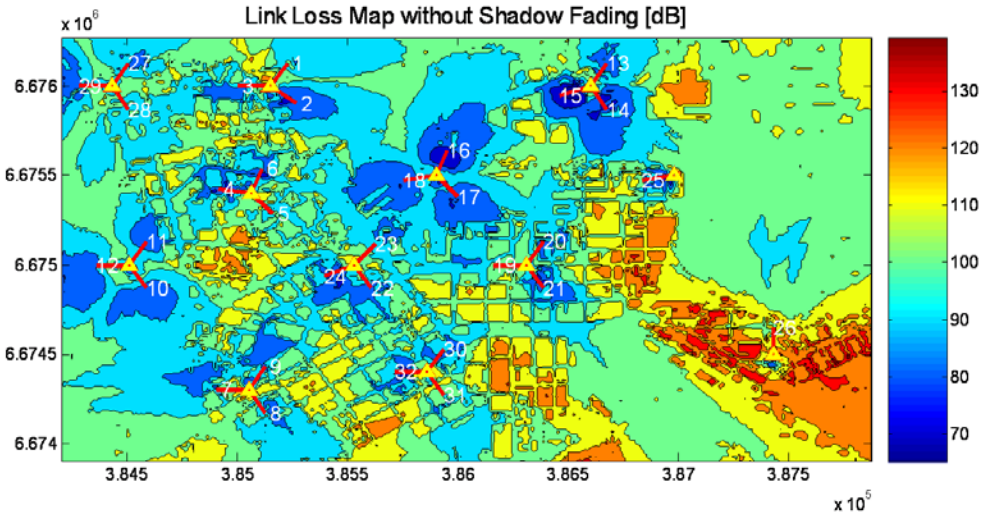

Figure 53. Link loss map of Helsinki downtown (no shadow fading case)

In the handover modeling of the snap-shot LTE simulator, a UE, that meets the following conditions (18 and 19), defined as a user which is going to perform a handover with a 50% probability.

$$RSRP_{imbalance} \cong 3.0\ dB \tag{18}$$

$$SINR_{source\ cell} \geq 6.0\ dB \tag{19}$$

In the simulator, RSRP reporting is modeled based on the conditions described in [TS36.133]. Furthermore, the probable SINR and RSRP values of the source and target cells are inquired in the zone of the performed handover which is determined based on a 10 km/h user movement assumption so that mobility related problems (e.g., handover drop) may be identified as well.

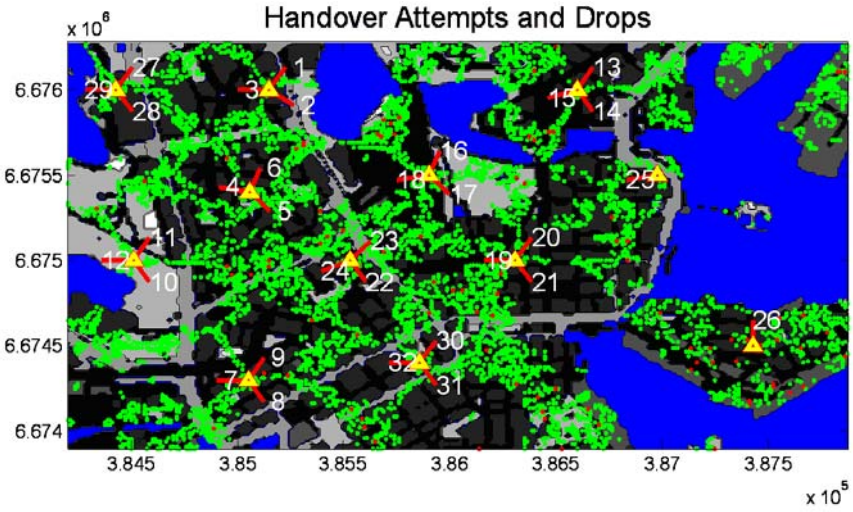

Figure 54. Handover attempt and drop locations before optimization

In addition to the reporting of RSRP and the identification of mobility related problems with root causes, Channel State Information (CSI) reporting, event-triggered and periodic UE reports, fault reports, alarms, among other things, have been implemented in the simulator. Measurement errors are also considered in simulations applying a normal distribution with the mean and standard deviation parameters that are modeled having regard to the accuracy requirements in [TS36.133].

B. Main Simulation Assumptions and Scenarios

Simulations are carried out for two regular hexagonal network layout (Figure 55) scenarios where inter-site distances are 500 m (3GPP case 1) and 1732 m (3GPP case 3) respectively and one irregular network layout of Helsinki downtown. Parameters and assumptions follow those selected by 3GPP for performance evaluations of LTE and LTE-A technologies [TR25814, TR36.814].

Table 7. Main Simulation Assumptions in LTE DL

Parameter	**Modeling and Values**
Network layout	Total network elements: 91 eNBs, 273 cells Monitored network elements: 19 eNBs, 57 cells
System frequency	2000 MHz
System bandwidth	10 MHz
Number of PRBs	50
Frequency reuse factor	1
Propagation loss model	$L = 128.1 + 37.6 \log_{10}(R)$, R in kilometers
Penetration loss	20 dB
TX power per sector	46 dBm
MIMO configuration	SISO, 1x2 MRC (default), 2x2 MIMO SM & SFC
Horizontal HPBW	$\varphi_{3dB} = 70^{o}$
Vertical HPBW	$\theta_{3dB} = 10^{o}$
Antenna tower height	32 m
UE height	1.5 m
Shadowing STD	8 dB
Shadowing decorrelation	0.5 (sites), 1 (sectors)
Shadowing decorr. distance	50 m
Channel model	Typical Urban (TU)
Traffic model	Best-effort
Scheduling	Round Robin
User distribution	Uniform
Thermal noise per PRB	-121.4 dBm
TX cable loss	2 dB
RX antenna gain	0 dBi
RX body loss	0 dB
Thermal noise per PRB	-121.4 dBm
RX noise figure	9 dB

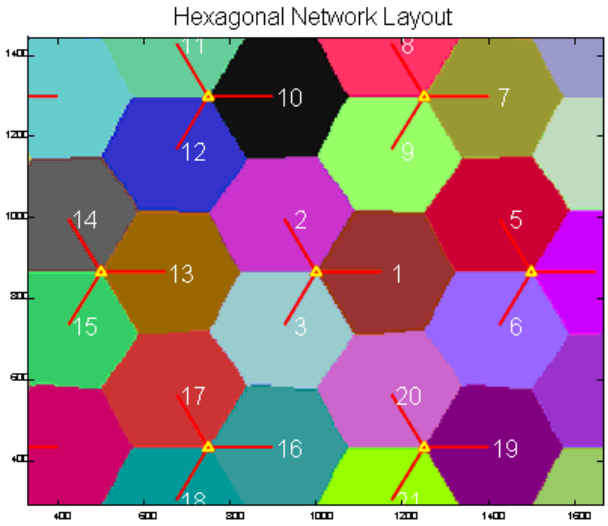

Figure 55. Regular hexagonal layout (no antenna elevation)

In simulations done for self-optimization studies, a 32-cell Helsinki downtown irregular network layout based on 3G WCDMA network planning scenario [Lai] is adopted as shown in Figure 56. Users are distributed with an elaborated traffic concentration modeling which takes into account user location (e.g., buildings, streets, water areas) in three dimensions. It is worth mentioning that LTE network planning and WCDMA network planning assumptions may differ from each other due to technical reasons (e.g., soft handover mechanism in WCDMA vs. hard handover mechanism in LTE).

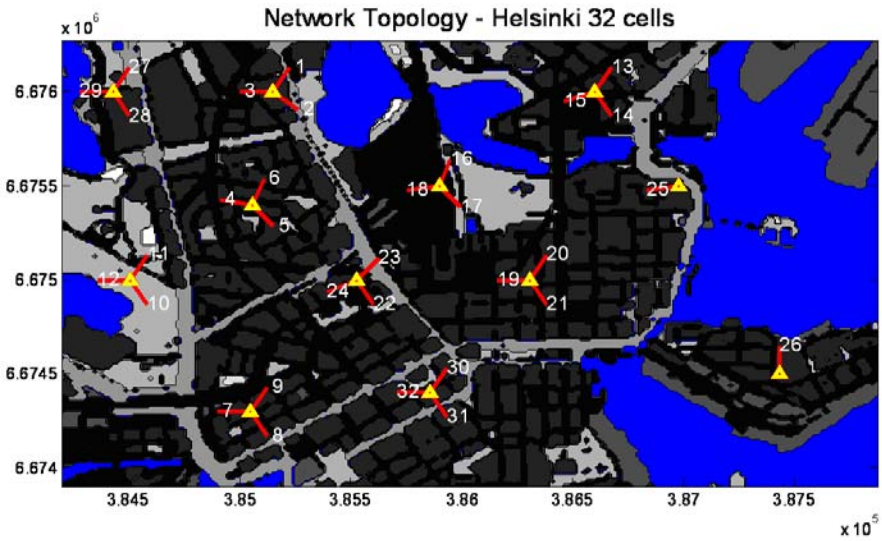

Figure 56. Network topology of Helsinki downtown

In performance evaluations, 5%-ile and 50%-ile of throughput and SINR Cumulative Distribution Functions (CDFs) are used as performance measures for coverage and capacity respectively.